Defensins mediate skin inflammation and itch in psoriasis

Sharan Kumar Balaji[1], Qin Zheng[2], Huasheng Yu[3], Joann Truong[1], Luchiano Giovanni Benjamin Fernando[1], Yining Liu[1], Clara Shin[3], Wenqin Luo[3], Xinzhong Dong[4] and Xintong Dong[1]

Journal of Investigative Dermatology (2026) ■, ■—■; doi:10.1016/j.jid.2026.08.014

Psoriasis is an inflammatory skin condition that features marked upregulation of keratinocyte-derived antimicrobial peptides, particularly β-defensins. Yet, the functions of these peptides in skin inflammation remain unclear. In this study, we used a defensin cluster-knockout mouse to evaluate the potential roles of defensins as neuroimmune modulators in psoriasis. Deletion of the defensin gene cluster (*Def* conditional knockout) in keratinocytes significantly attenuated imiquimod-induced psoriatic inflammation, with reduced hyperkeratosis, erythema, scaling, and expression of inflammatory cytokines and chemokines. In addition, the *Def* conditional-knockout mice exhibited reduced neutrophil and IL-17+ TCRγδ T-cell infiltration in the psoriatic skin, indicating a critical role of defensins in amplifying T helper 17 immunity. Behavioral analysis further revealed that the loss of defensins reduced psoriatic itch, and we showed that human β-defensin 2 directly activated small-diameter Mrgpra3 neurons to elicit robust scratching. Overall, our study revealed that β-defensins play an important role in mediating inflammation and itch associated with psoriasis by activating neutrophils, type 17 immune response, and pruriceptive sensory neurons, suggesting defensin signaling as a potential therapeutic target in psoriasis.

Keywords: β-Defensins, Inflammation, Itch, Neutrophils, Psoriasis

INTRODUCTION

Psoriasis is a chronic, immune-mediated inflammatory skin disorder that affects 2−3% of the population (Kamiya et al, 2019; Langley et al, 2005; Petit et al, 2021). It is characterized by erythema with plaques, keratinocyte (KC) hyperproliferation, neutrophil infiltration, and intense itch, all of which impact QOL (Orsmond et al, 2021; Vijayapoopathi et al, 2023; Zhang et al, 2025). The IL-23−IL-17 pathway plays a central role in driving psoriatic inflammation (Di Cesare et al, 2009; Potestio et al, 2024). IL-23 released by dendritic cells drives the differentiation and maintenance of T helper 17 cells, which produce IL-17 to promote KC hyperproliferation and cytokine release, establishing a self-amplifying inflammatory loop (Hu et al, 2021; Nussbaum et al, 2021; van der Fits et al, 2009). Clinical inhibitors targeting IL-23 and IL-17 have shown considerable efficacy (Ghoreschi et al, 2021; Griffiths et al, 2021), but the immune environment is highly complex and involves other modulators that vary with disease progression. Therefore, exploring multiple signaling pathways and additional immunogenic factors is essential for a more comprehensive understanding of psoriatic inflammation.

Among the genes most strongly upregulated in psoriatic skin are members of the defensin family, a group of small, positively charged, cysteine-rich antimicrobial peptides (AMPs) (Gao et al, 2021; Hollox et al, 2008; Lin et al, 2024; Morizane and Gallo, 2012; Xu and Lu, 2020). The first human beta-defensins, human β-defensin 2 (hBD2) and human β-defensin 3 (hBD3), were isolated from psoriatic skin (Harder et al, 2001, 1997), and hBD2 can serve as a biomarker for psoriasis because its levels are closely associated with the PASI score and respond quickly to anti−IL-17 treatment (Jansen et al, 2009; Kolbinger et al, 2017). Defensins are usually expressed at low levels in normal skin but are overexpressed in response to infection (Ali et al, 2001; Shelley et al, 2020; Sumikawa et al, 2006; Xu and Lu, 2020), injury (Butmarc et al, 2004), and inflammation (Shelley et al, 2020). During infection, pathogen-associated molecular patterns are detected by toll-like receptors on KCs and initiate intracellular signaling cascades that subsequently activate NF-κB, leading to the secretion of defensins and other proinflammatory mediators that aid in the clearance of pathogens (Froy, 2005; Gariboldi et al, 2008; Kumar et al, 2006; Vora et al, 2004). In psoriasis, however, despite

[1]Department of Biological Sciences, University of Texas at Dallas, Richardson, Texas, USA; [2]Department of Anesthesiology and Critical Care Medicine, Johns Hopkins University School of Medicine, Baltimore, Maryland, USA; [3]Department of Neuroscience, Perelman School of Medicine, University of Pennsylvania, Philadelphia, Pennsylvania, USA; and [4]Howard Hughes Medical Institute, Solomon H. Snyder Department of Neuroscience, Johns Hopkins University School of Medicine, Baltimore, Maryland, USA

Correspondence: Xintong Dong, Department of Biological Sciences, University of Texas at Dallas, Richardson, Texas 75080, USA. E-mail: Xintong.dong@utdallas.edu and Xinzhong Dong, Howard Hughes Medical Institute, Solomon H. Snyder Department of Neuroscience, Johns Hopkins University School of Medicine, Baltimore, Maryland 21205, USA. E-mail: xdong2@jhmi.edu

Abbreviations: AMP, antimicrobial peptide; CQ, chloroquine; DRG, dorsal root ganglion; hBD2, human β-defensin 2; hBD3, human β-defensin 3; IMQ, imiquimod; KC, keratinocyte; PMA, phorbol 12-myristate 13-acetate

Received 17 December 2025; revised 27 July 2026; accepted 14 August 2026; accepted manuscript published online XXX; corrected proof published online XXX

© 2026 Society for Investigative Dermatology. Published by Elsevier Inc. All rights are reserved, including those for text and data mining, AI training, and similar technologies.

there being no invading pathogens, KCs express high levels of defensins in response to IL-17 signaling (Furue et al, 2020). In addition to their antimicrobial activity, defensins have also been shown to perform immune modulatory roles, including the recruitment and activation of mast cells, neutrophils, dendritic cells, and T cells (Biragyn et al, 2002; Dong et al, 2022; Subramanian et al, 2013). Yet, despite their prevalence in psoriasis (Kolbinger et al, 2017; Tseng and Hoon, 2022), whether defensins contribute to disease pathogenesis and progression remains unclear.

To elucidate the roles of defensins in psoriasis, we utilized a defensin cluster knockout mouse model (denoted as *Def* cKO) (Dong et al, 2022). The defensin genes exhibit genetic and functional redundancy, making it difficult to confirm their roles through the knockout of individual defensins (Kolar et al, 2013; Morrison et al, 2002; Navid et al, 2012; Zhou et al, 2013). The mouse defensin gene cluster is located on chromosome 8 and spans over 3 million base pairs. To delete the entire cluster, 2 *loxp* sites were inserted into *Defb40* and *Defb13*, which are positioned at the 2 ends of the cluster. The Def^{flox} mice were bred with keratin14-cre (*K14*-cre) mice to conditionally knock out all defensins in the cluster from the KCs. A prior study demonstrated that the loss of defensins resulted in dysbiosis of the skin microbiome, leading to increased *Staphylococcus* colonization and severely impaired neutrophil-mediated clearance of *S aureus* (Dong et al, 2022).

In this study, using *Def* cKO mice, we show that ablation of defensins reduces psoriatic inflammation. Mice without defensins show reduced neutrophils and IL-17–producing T cells. Furthermore, we show that defensins contribute to psoriatic itch by directly activating itch sensory neurons. Collectively, these findings highlight the neuroimmune modulatory roles of defensins in mediating psoriatic inflammation and itch.

RESULTS

Defensins are highly expressed by a subpopulation of inflamed KCs in psor patients with psoriasis

The increased expression of defensins in psoriasis is well-documented (Harder and Schröder, 2005; Jansen et al, 2009; Štrajtenberger et al, 2024). Recent whole-transcriptome analyses of patient skin samples using single-cell and spatial technologies can further clarify the spatial pattern of defensin expression in psoriatic skin and the specific KC subpopulation that produces them. We analyzed publicly available human bulk RNA sequencing (GSE121212) (Tsoi et al, 2019), single-cell RNA sequencing (GSE151177) (Kim et al, 2021), and spatial transcriptomics (GSE202011) (Castillo et al, 2023) datasets to determine the location and transcriptomic features of defensin-producing KCs in psoriatic lesions. Bulk RNA-sequencing analyses confirmed that human β-defensin genes *DEFB4A* and *DEFB103B*, which encode hBD2 and hBD3, are among the most highly and significantly upregulated genes in psoriatic skin compared with healthy control groups (Supplementary Figure S1a) (Harder et al, 2001; Jansen et al, 2009). We then analyzed the gene expression features of defensin-producing cells using an RNA-sequencing dataset (Kim et al, 2021). Following the data analysis pipeline used in the original paper, we created a Uniform Manifold Approximation and Projection and categorized the cells into 12 clusters (Figure 1a and Supplementary Figure S1c). These include various immune cell types (CD4 T cells, CD8 T cells, T regulatory cells, mature and semimature dendritic cells), melanocytes, and 4 major subclusters of KCs (Stratum basale, Stratum granulosum, Stratum spinosum, and Stratum corneum). We found that *DEFB4A* and *DEFB103B* are expressed by a subpopulation of inflamed KCs in patients with psoriasis (Figure 1b). Furthermore, we subclustered the *DEFB4A*-expressing cells from the KCs that do not express *DEFB4A* among patients with psoriasis and controls. We found that *DEFB4A*-positive KCs in psoriasis also express other antimicrobial proteins, including S100 and small proline-rich region proteins, as well as the inflammatory cytokine IL-36 (Figure 1c).

Next, we analyzed the spatial transcriptomics dataset to map the spatial distribution of these inflamed KCs in psoriatic skin. We performed dimensionality reduction and harmony-based integration analyses and annotated 9 distinct cell clusters on the basis of marker genes used in the original study (Castillo et al, 2023). We found that *DEFB4A* expression was enriched specifically in inflamed suprabasal KCs in psoriatic skin and was not detected in healthy skin (Figure 1d). Using violin plot and spot-level correlation analyses, we found that the normalized expression of the suprabasal marker *K10* (keratin 10) and *DEFB4A* showed a partial but statistically significant positive association across tissue-associated spots (Spearman's rho = 0.441, $P = 2.21 \times 10^{-20}$). These findings support a partial spatial overlap between *K10*- and *DEFB4A*-expressing KCs (Supplementary Figure S2a and b). In summary, these analyses demonstrate that defensins are significantly overexpressed in human psoriatic skin, and these defensin genes are produced by a specific subpopulation of inflamed suprabasal KCs that may play a role in the inflammation associated with psoriasis.

Defensins mediate psoriatic inflammation

To elucidate the functions of defensins in psoriatic inflammation, we utilized a mouse model to induce psoriasis-like inflammation through the topical application of imiquimod (IMQ) cream on the nape of both *Def* cKO (Figure 2a) and wild-type (WT) mice for 7 days (Kusuba et al, 2018; Sakai et al, 2016; van der Fits et al, 2009; Wang et al, 2015). RNA-sequencing analysis (GSE161084) (Zhang et al, 2021) confirmed that, similar to human patients with psoriasis, IMQ-treated WT mouse skin showed a marked elevation in the expression of *Defb4* and *Defb14*, homologs of hBD2 and hBD3 (Supplementary Figure S1b). To validate the successful deletion of *Defb* genes in the *Def* cKO mouse model, we extracted RNA from WT control, 7-day IMQ-treated WT, *Def* cKO control, and 7-day IMQ-treated *Def* cKO skin and performed qPCR. Consistent with previous RNA-sequencing results (Merleev et al, 2022; Zhang et al, 2021), IMQ-treated WT skin showed a significant increase in *Defb2*, *3*, *4*, 6, and *14* gene expressions compared with WT controls, whereas *Defb1* was consistently expressed in both WT controls and IMQ-treated WT skin. In contrast, *Def* cKO control and IMQ-treated *Def* cKO mice showed almost no expression of any *Defb* genes (Figure 2b).

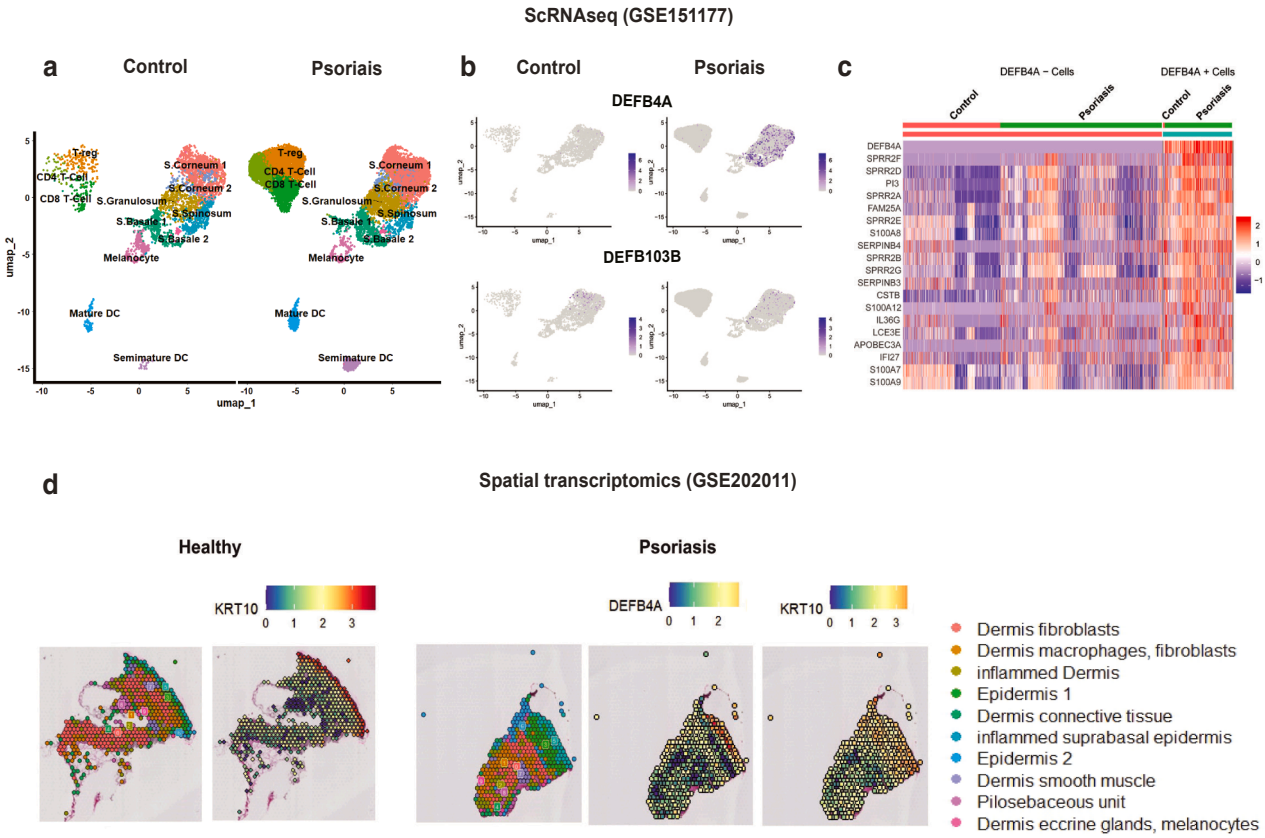


Figure 1. Defensins are highly expressed by inflamed suprabasal keratinocytes in human psoriatic skin. (**a**) UMAP analysis of published scRNA-seq data (GSE151177) showing major immune and keratinocyte subclusters from control and psoriatic skin. (**b**) Feature plots of *DEFB4A* and *DEFB103B*, demonstrating increased expression in keratinocyte subclusters in psoriatic skin. (**c**) Subclustering of keratinocytes into *DEFB4A*− and *DEFB4A*+ populations. The heatmap shows that *DEFB4A*+ cells coexpress *S100*, *SPRR*, and *IL-36*. (**d**) Spatial transcriptomics (GSE202011), identifying epidermal and dermal subclusters. *DEFB4A* expression localizes to inflamed suprabasal keratinocytes in psoriatic but not in healthy skin. Keratin 10 (*K10*) marks the suprabasal layer. scRNA-seq, single-cell RNA sequencing; UMAP, Uniform Manifold Approximation and Projection.

To determine whether murine defensins are expressed by suprabasal KCs, as observed in human psoriasis, we performed RNA FISH on IMQ-treated skin. We selected *Defb4* and *Defb14* for this study because they are homologs of *DEFB4* and *DEFB103*, which are known to be elevated in human psoriatic skin. Owing to the short length of *Defb4* transcripts, we used BaseScope to chromogenically visualize *Defb4* transcripts in WT control, IMQ-treated WT, *Def* cKO control, and IMQ-treated *Def* cKO skin. IMQ-treated WT skin showed significantly elevated expression of *Defb4* (Figure 2c, blue dots) in the suprabasal layer of the epidermis compared with controls, whereas no transcripts were detected in control or IMQ-treated *Def* cKO skin. Similarly, *Defb14* was probed using hybridization chain reaction RNA FISH in both WT control and IMQ-treated WT skin. We also found *Defb14* transcripts in the suprabasal epidermal layer in IMQ-treated WT skin compared with that in the controls (Figure 2d), and the signal was completely abolished in the *Def* cKO animals.

Next, we phenotypically compared the levels of skin inflammation in WT and *Def* cKO mice after IMQ treatment. IMQ-treated *Def* cKO mice exhibited a marked reduction in scaling compared with IMQ-treated WT mice (Figure 2e and h). We quantified disease severity by daily measurements of skin thickness and the cumulative psoriasis severity index, which is a combination of erythema and scaling scores. IMQ-treated *Def* cKO mice showed a significant reduction in skin thickness compared with their IMQ-treated WT counterparts starting from day 3 ($P < .0001$) and demonstrated significantly lower erythema scores from day 1 ($P < .0001$), reduced scaling from day 4 ($P < .0067$), and decreased _cumulative scores from day 1 ($P < .0008$) compared with IMQ-treated WT animals (Figure 2f–i). We also validated these results by applying IMQ to mouse ears. Consistent with the nape skin model, IMQ-treated *Def* cKO mice showed reduced ear thickness beginning on day 4 compared with IMQ-treated WT mice (Supplementary Figure S3a and b). We subsequently performed a histological assessment by H&E staining, further confirming a reduction in total skin thickness (epidermal and dermal) in IMQ-treated *Def* cKO animals ($P = .0223$) compared with that in WT mice (Figure 2j), supporting the conclusion that *Def* cKO mice exhibit reduced psoriatic inflammation. Overall, these findings show that defensins produced by inflamed suprabasal KCs contribute to IMQ-driven psoriatic inflammation.

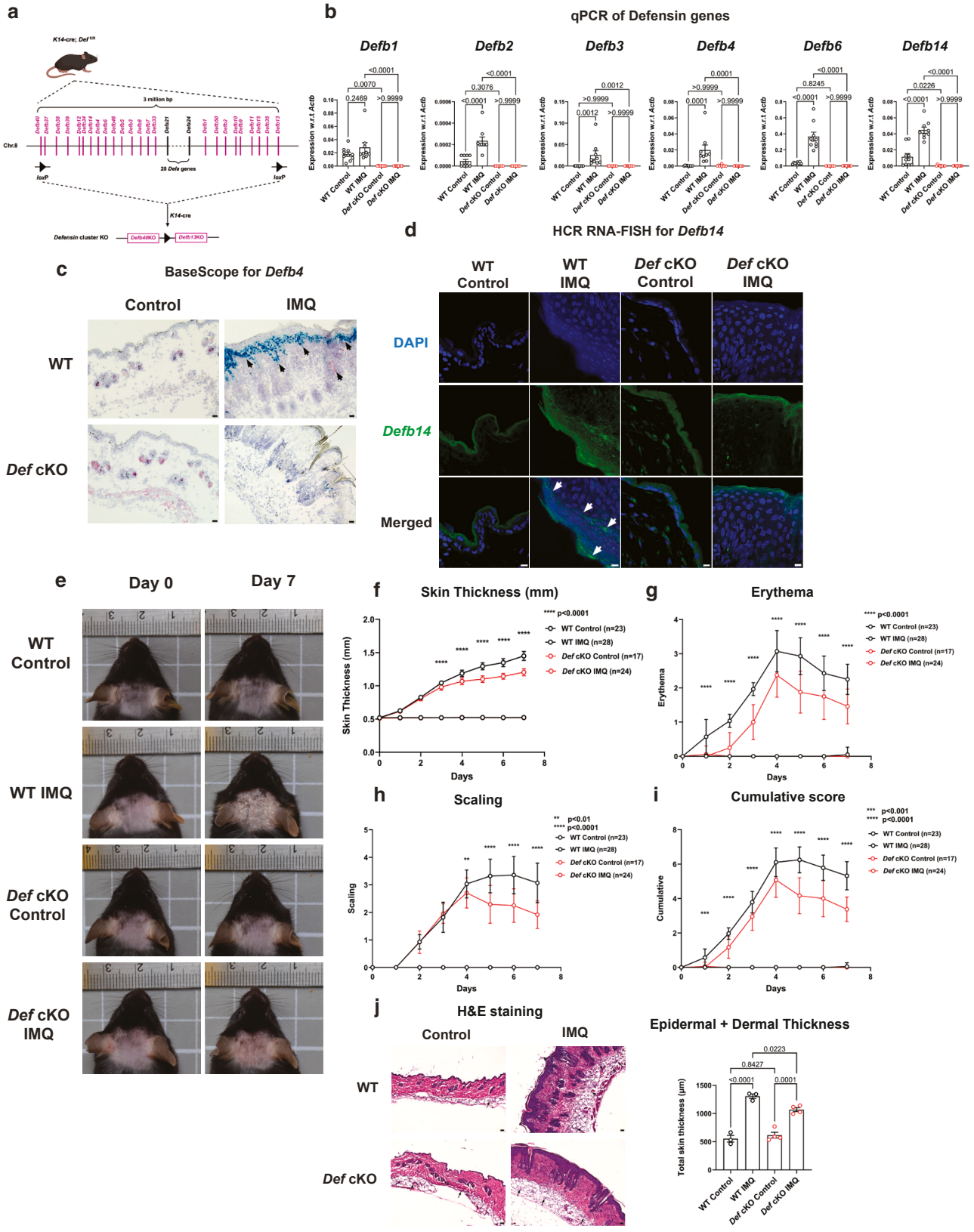


Figure 2. Defensins are required for psoriasis-like inflammation. (**a**) Schematic of keratinocyte-specific *Def* cKO (defensin cluster knockout) mice generated by inserting loxP sites flanking the β-defensin locus and crossing with *K14*-cre. (**b**) qPCR of β-defensin genes in WT (black) and *Def* cKO (red) control skin and 7 days after IMQ treatment. (**c**) BaseScope showing *Defb4* (blue) in suprabasal epidermis of IMQ-treated WT skin and *K16* (red) in dermis. Bar = 50 μm. (**d**) HCR RNA-FISH of *Defb*14 (green puncta) in IMQ-treated WT skin, not in *Def* cKO skin. Nuclei were labeled with DAPI. Bar = 10 μm. (**e**) Representative images of the shaved nape skin of control and IMQ-induced skin. (**f**–**i**) Quantification of skin thickness, erythema, scaling, and cumulative scores over 7 days. (**j**) H&E staining and quantification of total skin thickness (n = 3). Bar = 50 μm. Data are presented as mean ± SD. $^{**}P < .01$, $^{***}P < .001$, and $^{****}P < .0001$. One-way

IMQ treatment alters the skin microbiome in WT and *Def* cKO mice

Given the antimicrobial function of defensins, we examined whether changes in the skin microbiome could contribute to the reduced IMQ-induced inflammation observed in *Def* cKO mice. To address this, we analyzed the skin microbiome of WT and *Def* cKO mice under control and IMQ-treated conditions. Mice were weaned and housed with littermates of the same genotype for 7 weeks before IMQ treatment. Skin swabs were then collected from the nape skin and analyzed by 16S ribosomal RNA sequencing (Bolyen et al, 2019; Fyhrquist et al, 2019; Grogan et al, 2019). Beta diversity analysis showed that WT and *Def* cKO control samples clustered closely together, whereas IMQ-treated WT and *Def* cKO samples had distinct microbiomes (Supplementary Figure S4a). Alpha diversity, as measured by Shannon indices, was significantly reduced after IMQ treatment in both WT and *Def* cKO mice, indicating that IMQ-induced inflammation is associated with a loss of microbial diversity. However, Shannon diversity was not significantly different between IMQ-treated WT and *Def* cKO samples (Supplementary Figure S4b). Taxonomic analysis showed that IMQ-treated WT mice had an increased relative abundance of *Staphylococcus*, whereas IMQ-treated *Def* cKO mice showed an increased relative abundance of *Staphylococcus*, *Streptococcus*, and *Corynebacterium* (Supplementary Figure S4c). Together, these findings indicate that IMQ treatment induces marked changes in the skin microbiome in both WT and *Def* cKO mice, but the reduction in microbial alpha diversity occurs in both WT and *Def* cKO mice and therefore does not alone explain the reduced inflammatory phenotype observed in *Def* cKO animals.

Defensins mediate neutrophil infiltration in psoriasis

To understand how defensin loss of function alters the immune environment in psoriatic skin, we examined the expression of key proinflammatory mediators associated with psoriasis. qPCR analysis revealed that IMQ-treated *Def* cKO skin exhibited a marked reduction in the expression of neutrophil-associated genes, including *Il1b*, *Cxcl2*, *Tnf*, *S100a8*, and *S100a9*, compared with IMQ-treated WT skin (Figure 3a) (Man et al, 2023; Sato et al, 2020; Sieminska et al, 2024). These findings suggest that defensins may contribute to psoriasis by promoting neutrophilic inflammation.

The accumulation of neutrophils in microabscesses within the epidermis is a key feature of psoriasis (Chiang et al, 2019). We next investigated whether defensins influence neutrophil recruitment in IMQ-treated skin after day 7 using flow cytometry. Neutrophils were gated as CD45+ CD11b+Ly6g+ cells (Figure 3b). IMQ-treated *Def* cKO skin showed a significant decrease in the percentage of neutrophils compared with IMQ-treated WT skin ($P < .0001$) (Figure 3b), which correlates with lower expression of neutrophil-specific genes (Figure 3a). To further validate these findings histologically, we performed immunofluorescence staining using an anti-Ly6g antibody on WT control, IMQ-treated WT, *Def* cKO control, and IMQ-treated *Def* cKO skin. We quantified the number of Ly6g+ cells in both the epidermis and the full skin. Consistent with the flow cytometry results, IMQ-treated *Def* cKO skin showed a significant decrease in the overall count of Ly6g+ cells compared with IMQ-treated WT skin (Figure 3c). Furthermore, Ly6g+ cells in the epidermis were also reduced in IMQ-treated *Def* cKO mice compared with that in WT mice. Taken together, these results demonstrate that defensins are crucial mediators of neutrophil recruitment and accumulation in psoriatic skin. The loss of defensins in *Def* cKO mice impairs neutrophil infiltration, reduces inflammation, and reduces epidermal microabscess formation, highlighting the crucial role of defensins in driving neutrophilic inflammation in psoriasis.

Defensins induce IL-17 secretion from neutrophils and mediate IL-17+ TCRγδ T-cell infiltration in psoriasis

IL-17 and IL-23 are essential cytokines involved in the progression of psoriasis. Our qPCR results showed that IMQ-treated *Def* cKO animals exhibited significant downregulation of *Il17a*, *Il17f*, and *Il23* compared with IMQ-treated WT animals (Figure 3a). Previous studies have shown that neutrophils can serve as a source of IL-17 in psoriatic lesions and other inflammatory conditions (Dyring-Andersen et al, 2017; Li et al, 2010; Lin et al, 2011). To investigate whether defensins can stimulate IL-17 release from neutrophils, we cultured bone marrow–derived neutrophils from WT mice and stimulated them with recombinant hBD2 and hBD3 (10 μM) for 12 hours (McGill et al, 2021). We then collected the supernatants and performed an ELISA. Our findings revealed that cultured bone marrow neutrophils showed a significant increase in IL-17 secretion upon stimulation with hBD3 and lipopolysaccharide, which was used as a positive control (Ferretti et al, 2003; Hu et al, 2017) (Figure 3d). Because neutrophils are short lived and susceptible to cell death during prolonged culture, we wanted to determine whether IL-17 release was due to neutrophil activation upon hBD3 stimulation or due to cell death. To assess cytotoxicity, bone marrow–derived neutrophils were stimulated with hBD2, hBD3, lipopolysaccharide, or phorbol 12-myristate 13-acetate (PMA). PMA was included as a positive control because it induces NETosis (Inozemtsev et al, 2023). Lactate dehydrogenase analysis showed that 12-hour treatment with lipopolysaccharide, hBD2, or hBD3 increased cytotoxicity compared with unstimulated controls; however, the magnitude of lactate dehydrogenase release was substantially lower than that induced by PMA (Supplementary Figure S5), and stimulation with PMA did not show any significant increase in IL-17 levels (Figure 3d), suggesting that the IL-17 detected by ELISA after hBD3 treatment was not primarily due to cell death and instead was consistent with hBD3-mediated neutrophil activation.

To evaluate the effects of defensin loss of function on T-cell populations, we performed flow cytometry analyses to quantify total T cells (CD3+), CD4+, CD8+, and TCRγδ T-cell populations. We were particularly interested in IL-17+ TCRγδ T cells, because this population was known to be expanded in psoriasis by responding to IL-23, producing IL-

and 2-way ANOVA were used to calculate the *P*-values. Sidak's and Tukey's multiple-comparison posthoc tests were used. WT, wildtype; IMQ, Imiquimod; HCR, hybridization chain reaction; WT, wild-type.

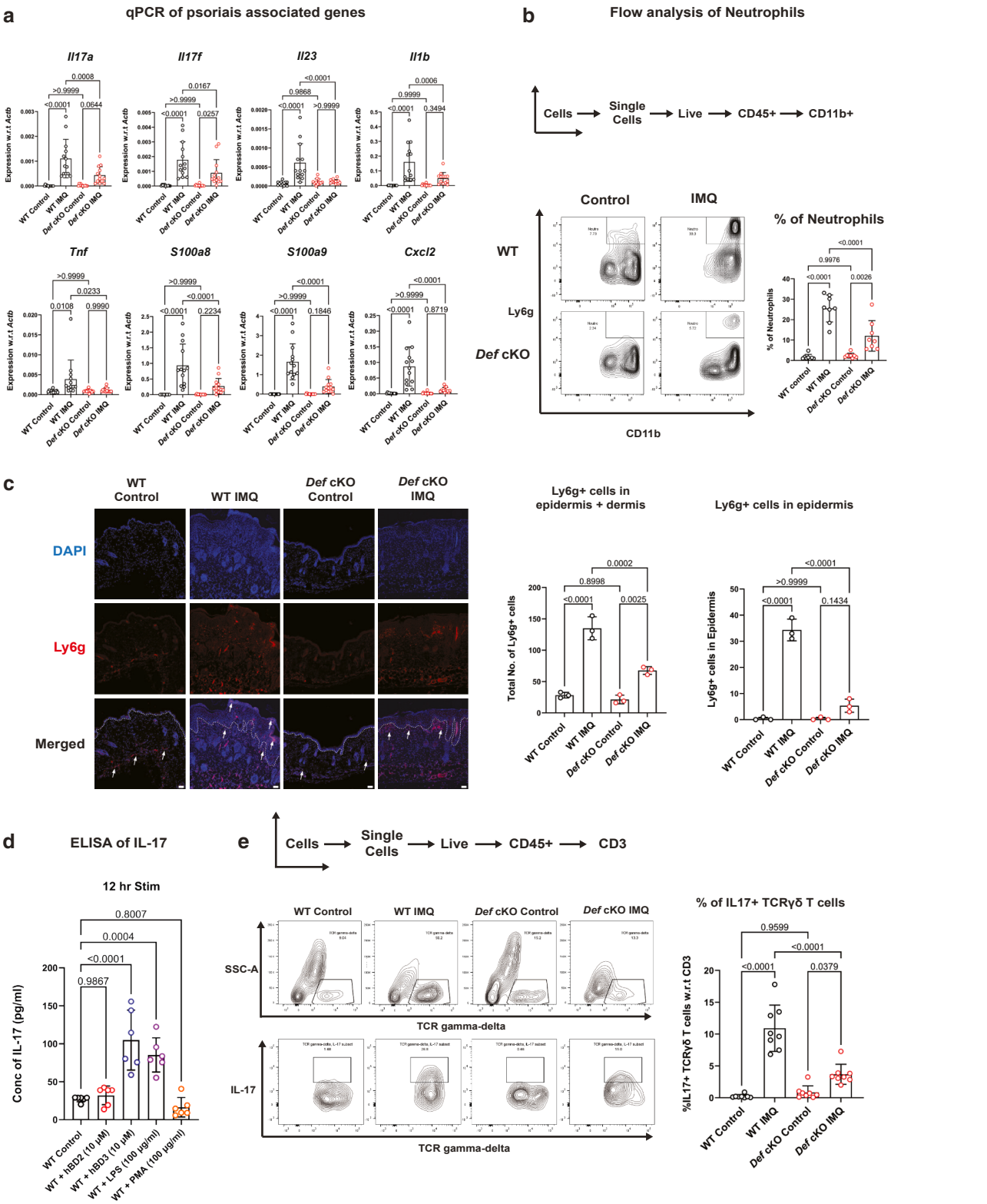


Figure 3. Defensins promote neutrophil recruitment and IL-17+ TCRγδ T-cell infiltration in psoriasis. (**a**) qPCR analysis of proinflammatory (*Il17a*, *Il17f*, *Il23*, and *Tnf*) and neutrophil-associated (*Il1b*, *S100a8*, *S100a9*, and *Cxcl2*) genes in WT and *Def* cKO control and after 7 days of IMQ treatment (n = 13). (**b**) Flow cytometry analysis of neutrophils from WT control, WT IMQ, *Def* cKO control, and *Def* cKO IMQ-treated skin. The gating strategy of live $CD45^+CD11^+Ly6g^+$ neutrophils is shown. The quantification of neutrophil percentage is shown on the right (n = 8). (**c**) Immunofluorescence images of $Ly6g^+$ neutrophils (red) in WT control, WT IMQ, *Def* cKO control, and *Def* cKO IMQ-treated skin. Nuclei are labeled with DAPI. The quantification of total $Ly6G^+$ cells in the skin and $Ly6G^+$ cells within the epidermis is shown on the right. The dotted line indicates the epidermis, with arrows pointing to the infiltrated neutrophils (n = 3). Bar = 50 µm. (**d**) ELISA for IL-17 from the supernatant of bone marrow–derived neutrophils stimulated with LPS (100 µg/ml), hBD2 (10 µM), hBD3 (10 µM), and PMA (100 µg/ml) for 12 hours (n = 6). (**e**) Flow cytometry analysis of IL-17+ TCRγδ T cells in WT and *Def* cKO IMQ-treated skin. The quantification of total IL-17+ TCRγδ T-cell percentage with respect to CD3 is shown on the right. (n = 8). Data are presented as mean ± SD. One-way

17, and driving inflammation (Cai et al, 2011; Qi et al, 2021). We found that IMQ-treated *Def* cKO animals exhibited a significant decrease in the percentage of IL-17+ TCRγδ T cells compared with IMQ-treated WT animals (Figure 3e), whereas no changes were observed in the other T-cell populations (Supplementary Figure S6a–d). These results lead to an overall model where defensins promote IL-17 production by neutrophils and facilitate the infiltration of IL-17+ TCRγδ T cells, thereby amplifying the IL-17 signaling pathway and exacerbating inflammation in psoriasis.

Defensins activate Mrgpra3 neurons to mediate psoriatic itch

Itch is a common symptom among individuals with psoriasis and tends to worsen as the disease progresses (Elewski et al, 2019; Komiya et al, 2020; Yosipovitch et al, 2018). Interestingly, defensins have been shown to activate members of the Mrgpr (Mas-related G-protein-coupled receptor) family—particularly Mrgpra3 and Mrgprc11—which are expressed in sensory neurons responsible for itch (Bader et al, 2014; Liu et al, 2009; McNeil and Dong, 2014; Meixiong et al, 2019; Tseng and Hoon, 2022; Zhang and McNeil, 2019). Therefore, we sought to determine whether defensins mediate itch associated with psoriasis. We treated the nape skin of both WT and *Def* cKO mice with IMQ for 7 days and recorded the animals' scratching behavior. Itch behavior was quantified by both manual counting of scratch bouts over a 30-minute period and by an automated machine-learning algorithm, ScratchAID (Yu et al, 2022). Notably, we observed that *Def* cKO mice treated with IMQ exhibited less scratching behavior than WT mice (Figure 4a and b).

We next investigated whether Mrgpra3+ neurons are crucial for defensin-mediated psoriatic itch using a *Mrgpra3*^{DTA} mouse model, in which all Mrgpra3+ neurons are selectively ablated through Cre-dependent expression of diphtheria toxin subunit A. *Mrgpra3*^{DTA} mice subjected to IMQ showed a marked decrease in itch behavior compared with WT mice (Figure 4c). ScratchAID-based quantification further showed that IMQ-treated *Mrgpra3*^{DTA} mice exhibited significantly reduced total scratch time compared with WT mice, consistent with the manual scratch bouts (Figure 4d). Next, we directly assessed the ability of defensins to cause itch by administering mBD4, hBD2, and hBD3 peptides intradermally into the cheeks of WT and *Mrgpra3*^{DTA} mice. We used human defensins hBD2 and hBD3 because they are functional homologs of mBD4 and mBD14, and prior studies have shown that human β-defensins can activate mouse Mrgpr receptors, which are homologous to human MRGPRs, with similar half maximal effective concentration values (Dong et al, 2022; Tseng and Hoon, 2022; Zhang et al, 2026). Consistent with previous reports (Tseng and Hoon, 2022; Zhang and McNeil, 2019), mBD4, hBD2, and hBD3 elicited scratching responses in the WT mice, whereas the ablation of Mrgpra3+ neurons significantly reduced both the scratch bouts and the total scratch time in response to defensin injections, supporting our hypothesis that defensins trigger itch by activating Mrgpra3+ neurons (Figure 4e–j). To further assess whether defensins activate sensory neurons directly to provoke itch or do so indirectly through immune cell activation, we isolated dorsal root ganglion (DRG) neurons from *Pirt*^{Salsa} mice, in which all DRG neurons express a TdTomato marker and a genetically encoded calcium indicator GCaMP6f, and stimulated the neurons with hBD2. This in vitro calcium imaging experiment demonstrated that hBD2 activated small-diameter neurons (Figure 5a). Among the hBD2-activated neurons, 41.97 ± 15.99% of neurons also responded to the Mrgpra3 agonist chloroquine (CQ) (Figure 5a and b). We also examined the overlap between hBD2-responsive neurons and the NP1/MrgprD+ neurons, which are activated by β-alanine and have been implicated in itch and pain (Guo et al, 2023; Liu et al, 2012), as well as NP3/serotonin-responsive neurons, which are also involved in itch signaling (Cevikbas and Lerner, 2020). In vitro calcium imaging showed that smaller portions of hBD2-responsive neurons also responded to β-alanine (16.16 ± 8.66%) or serotonin (19.05 ± 17.98%) (Supplementary Figure S7a–d). Together, these 3 itch neuron populations account for roughly 77% of all hBD2-responsive neurons, indicating that itch is the primary sensory modality activated by hBD2. Similarly, we also isolated DRG from WT and *Mrgpra3*^{DTA} mice and performed calcium imaging with Fluo-4, a dye that measures intracellular calcium. We found that the total number of hBD2-activated neurons was reduced in the *Mrgpra3*^{DTA} mice compared with that in WT mice (Figure 5c and Supplementary Figure S8a), supporting the notion that hBD2 directly activates Mrgpra3+ neurons. We further assessed the ability of defensins to activate sensory neurons using in vivo calcium imaging by injecting hBD2 and CQ into the hind paw of *Pirt*^{GCaMP6s} mice, which express the genetically encoded calcium ion indicator GCaMP6s in all DRG neurons. Using in vivo calcium imaging of the lumbar 4 DRG, we observed that hBD2 elicited robust neuronal activation. Notably, 62.89 ± 15.98% of hBD2-responsive neurons also responded to CQ, indicating substantial overlap with the Mrgpra3-positive pruriceptive population and supporting our in vitro findings (Figure 5d). Together, these results show that hBD2 can elicit itch by directly activating the Mrgpra3+ NP2 itch neurons. These results are consistent with the proposed role of defensins as itch mediators (Tseng and Hoon, 2022).

Next, we investigated the localization of defensin-expressing KCs with respect to Mrgpra3+ neurons innervating the skin. We performed hybridization chain reaction RNA FISH for *Defb14* on IMQ-treated *Mrgpra3*^{Tdtomato} mice, in which Mrgpra3+ nerve terminals in the skin are visualized with Tdtomato. We found that *Defb14* transcripts were localized near Mrgpra3+ neurons, confirming that these peptides can potentially interact directly with itch sensory neurons (Supplementary Figure S8b). Previous research has shown that activated Mrgpra3+ neurons can secrete neuropeptides and regulate skin immunity (Inclan-Rico et al, 2024). To determine whether Mrgpra3^{+} neurons are necessary for psoriatic inflammation, we investigated IMQ-treated *Mrgpra3*^{DTA} mice, in which Mrgpra3^{+} neurons are selectively ablated. These

ANOVA was used to calculate the *P*-values. hBD2, human β-defensin 2; hBD3, human β-defensin 3; IMQ, imiquimod; LPS, lipopolysaccharide; PMA, phorbol 12-myristate 13-acetate; WT, wild-type.

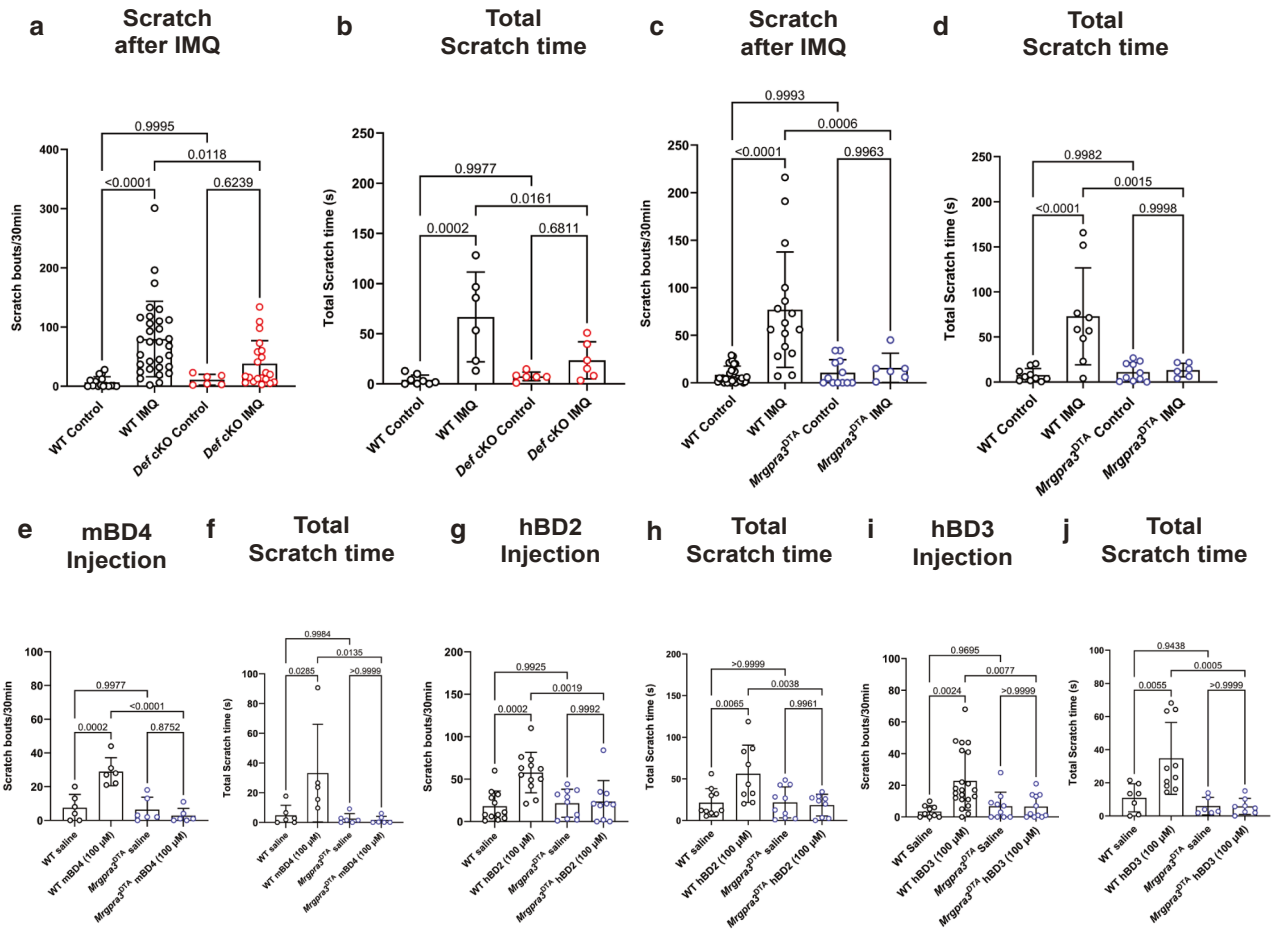


Figure 4. Defensins activate Mrgpra3 neurons to mediate psoriatic itch. (**a**) Quantification of scratching behavior in WT (black) and *Def* cKO (red) mice treated with IMQ for 7 days. Scratch bouts were counted manually for 30 minutes (n = 6–31). (**b**) Total scratch time analysis of WT and *Def* cKO mice after 7 days of IMQ treatment using ScratchAID. The time was calculated using 30 frames per second (n = 6–8). (**c**) Quantification of itch behavior in WT (black) and *Mrgpra3* neuron-ablated mice (*Mrgpra3*^{DTA}) (blue) after 7 days of IMQ treatment. Scratch bouts were counted manually for 30 minutes (n = 6–31). (**d**) Total scratch time analysis of WT and *Mrgpra3*^{DTA} mice after 7 days of IMQ treatment using ScratchAID (n = 6–10). (**e**) Cheek injection of mBD4 (100 μM) in WT and *Mrgpra3*^{DTA} mice, and scratch bouts were counted for 30 minutes (n = 6). (**f**) Total scratch time analysis of WT and *Mrgpra3*^{DTA} mice after mBD4 (100 μM) cheek injection using ScratchAID (n = 5–6). (**g**) Cheek injection of hBD2 (100 μM) in WT and *Mrgpra3*^{DTA} mice, and scratch bouts were counted for 30 minutes (n = 10–12). (**h**) Total scratch time analysis of WT and *Mrgpra3*^{DTA} mice after hBD2 (100 μM) cheek injection using ScratchAID (n = 9–10). (**i**) Cheek injection of hBD3 (100 μM) in WT and *Mrgpra3*^{DTA} mice (n = 9–21). (**j**) Total scratch time analysis of WT and *Mrgpra3*^{DTA} mice after hBD3 (100 μM) cheek injection using ScratchAID (n = 6–10). Data are presented as mean ± SD. One-way ANOVA and Sidak's multiple comparison test were used to calculate the *P*-values. IMQ, imiquimod; hBD2, human β-defensin 2; hBD3, human β-defensin 3; mBD4, mouse β-defensin 4; WT, wild-type.

mice exhibited a mild but statistically significant reduction in skin thickness compared with IMQ-treated WT controls, but their psoriasis severity index scores were not significantly different (Supplementary Figure S9a–e), indicating a more specialized role for Mrgpra3^{+} neurons in mediating psoriatic itch rather than driving inflammation. Together, these results suggest that defensins directly activate Mrgpra3+ itch sensory neurons to induce psoriatic itch.'

DISCUSSION

In this study, we demonstrated that defensins secreted by inflamed KCs act as critical activators of immune cells and sensory neurons, driving psoriatic inflammation and itch. The immune-modulatory roles of defensins have been recognized for decades (Harder et al, 1997; Morizane and Gallo, 2012; Semple and Dorin, 2012; Yang et al, 1999). However, the functional significance of their increased expression in psoriasis has long remained unresolved owing to significant genetic redundancy within this locus (Morrison et al, 2002; Navid et al, 2012). By deleting the entire defensin cluster in KCs, we directly examined how the lack of these AMPs affects psoriatic inflammation and itch in vivo.

Our results showed that defensins are critical for the development of IMQ-induced psoriasis. *Def* cKO animals showed a significant reduction in epidermal hyperkeratosis, lower expression of inflammatory mediators, and reduced immune cell infiltration. Through transcriptomic analysis, we found that defensin expression is restricted to a distinct population of inflamed suprabasal KCs that coexpress AMPs, including S100 proteins, small proline-rich region proteins, and IL-36 family cytokines. These inflammatory molecules are well-established in the context of psoriatic inflammation and barrier stress (Foster et al, 2014; Hänel et al, 2013; Saito-Sasaki and Sawada, 2023; Tian et al, 2021). These AMP-

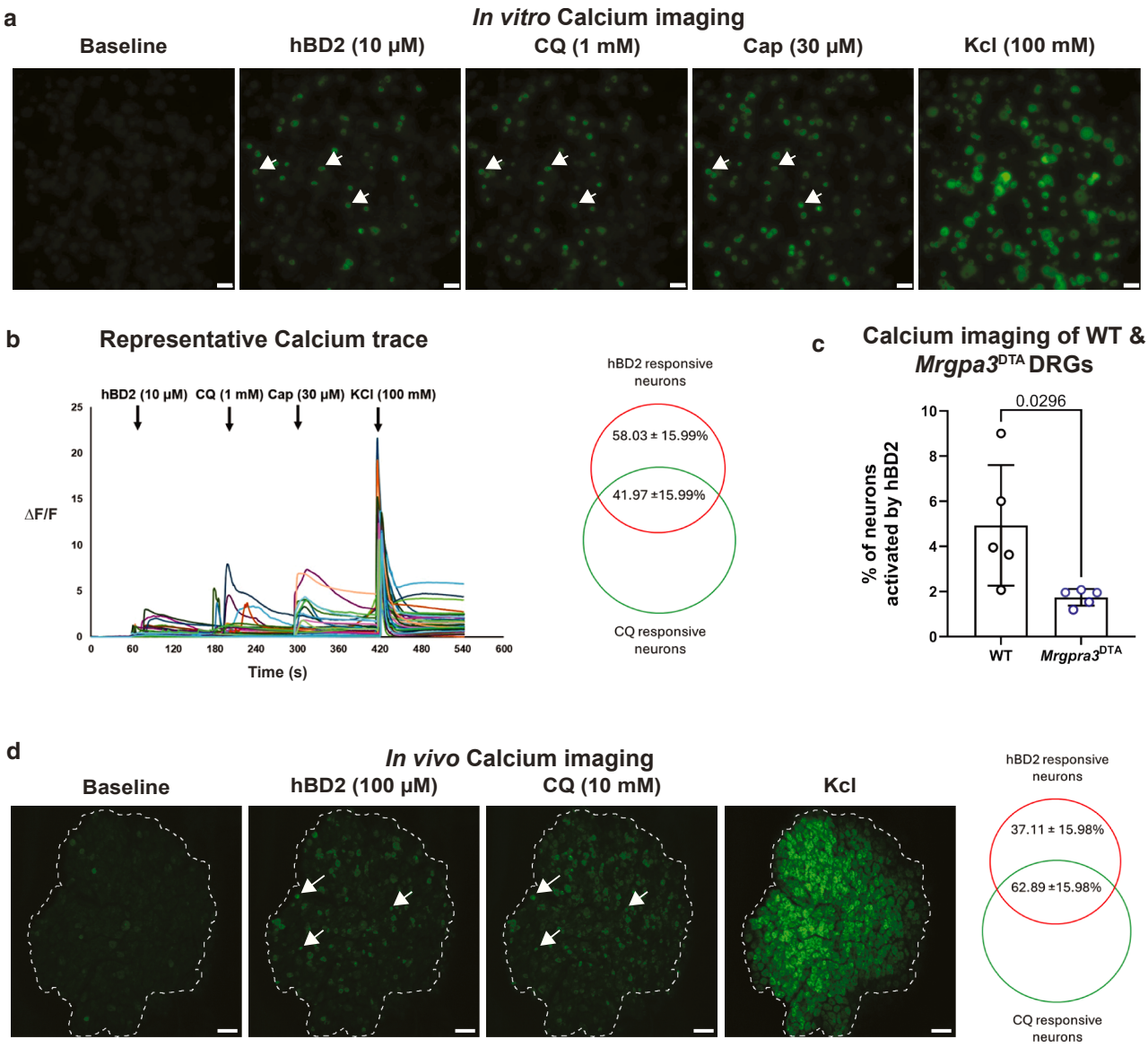


Figure 5. hBD2 directly activates Mrgpra3+ sensory neurons both in vitro and in vivo. (**a**) In vitro calcium images of cultured DRG neurons from *Pirt*^{Salsa} mice, which have a Gcamp6f (calcium indicator) genetically encoded. These neurons are stimulated with hBD2 (10 μM), CQ (1 mM), capsaicin (denoted as cap) (30 μM), and KCl (100 mM). Bar = 50 μm (n = 5). (**b**) Representative calcium trace of hBD2, CQ, and capsaicin-activated neurons. Arrows pointing at the neurons activated by hBD2, CQ, and capsaicin. ΔF/F cutoff for activation is 0.5. Venn diagram showing that among hBD2-activated neurons, 41.97 ± 15.99% responded to CQ. (**c**) In vitro calcium imaging of DRG neurons from WT and *Mrgpra3*^{DTA} mice. The neurons are labeled with Fluo-4 for 30 minutes and stimulated with hBD2 (10 μM), CQ (1 mM), capsaicin (denoted as cap) (30 μM), and KCl (100 mM) (n = 5). (**d**) In vivo calcium images of L4 DRG from *Pirt*^{Gcamp6s} after hind paw injection of hBD2 and CQ. Arrows point at the neurons activated by both hBD2 and CQ. hBD2 evoked a strong response, and ~63% of hBD2-responsive neurons also respond to CQ. Bar = 50 μm (n = 5). Data are presented as mean ± SD. Two-tailed *t*-test was used to calculate the *P*-values. CQ, chloroquine; DRG, dorsal root ganglion; hBD2, human β-defensin 2; KCl, potassium chloride; L4, lumbar 4; WT, wild-type.

expressing KCs within this spatially localized inflammatory niche are potentially important drivers of psoriatic pathology.

A previous study identified neutrophils as key effector cells of defensin (Dong et al, 2022). Neutrophils are abundant innate immune cells in circulation and perform a wide range of immune functions (Fox et al, 2010; Hermosilla et al, 2014; Kienle and Lämmermann, 2016; Radic and Marion, 2013). Neutrophils contribute to psoriatic inflammation by releasing cytokines, activating other immune cells, and forming neutrophil extracellular traps; their accumulation in Munro's microabscesses is a hallmark of the disease (Chiang et al, 2019; Czerwińska and Owczarczyk-Saczonek, 2022; Wang and Jin, 2020; Wang and Shi, 2023). We also found that the loss of defensins reduced neutrophil infiltration in the skin, revealing defensins as key epithelial signals that mediate neutrophil accumulation in psoriatic lesions.

Neutrophils also express IL-17 in inflammatory conditions (Dyring-Andersen et al, 2017; Li et al, 2010; Lin et al, 2011), and the IL-23/IL-17 axis is essential for the progression of psoriasis. T helper 17 cells are the major producers of IL-17A and IL-17F, which drive KC proliferation and promote the expression of cytokines and AMPs (Blauvelt and Chiricozzi,

2018; Martin et al, 2013; Mosca et al, 2021), creating a self-amplifying loop of inflammation. We found that defensins directly induce IL-17 production by neutrophils and that the percentages of IL-17+ TCRγδ T cells were lower in the skin of *Def* cKO animals after IMQ treatment. These results suggest that defensins affect both the innate and adaptive arms of the IL-23/IL-17 pathway, further emphasizing their importance as regulators of psoriatic inflammation.

In addition to modulating immune responses, defensins directly activate sensory neurons to drive psoriatic itch. Itch in psoriasis is among the most disruptive symptoms reported by patients with psoriasis, yet its mechanistic basis remains incompletely understood (Komiya et al, 2020; Taliercio et al, 2021). Previous studies have shown that β-defensins can activate sensory neurons through Mrgprc11 and Mrgpra3 in mice (Bader et al, 2014; Meixiong and Dong, 2017), but a direct role of defensins in psoriatic itch has not been demonstrated. In this study, we show that the loss of defensins substantially reduces scratching behavior and that genetic ablation of Mrgpra3 neurons mimics this effect.

Although *Def* cKO mice showed significantly reduced scratching after IMQ treatment, scratching was not completely abolished. This residual itch likely reflects the complex inflammatory environment of psoriatic skin. Previous studies have identified several itch mediators in psoriasis, including neuropeptides such as substance P and nerve GF, which can increase cutaneous nerve density and aggravate histamine-independent itch, and cytokines such as IL-31, TSLP, and IL-2. These mediators are elevated in lesional psoriatic skin and may contribute to itch independently of defensins (Komiya et al, 2020; Reich and Szepietowski, 2007). Thus, defensin-independent pruritogenic pathways likely remain active in *Def* cKO mice and contribute to the residual scratching observed after IMQ treatment. In contrast, hBD2-evoked scratching was strongly reduced in *Mrgpra3*^{DTA} mice, indicating that Mrgpra3+ neurons are the major neuronal pathway mediating acute defensin-induced itch.

Both in vivo and in vitro calcium imaging confirmed that human β-defensins activated small-diameter sensory neurons, many of which are Mrgpra3 responsive. These results align with earlier studies showing that Mrgpra3+ sensory neurons are primary pruriceptors in a variety of inflammatory skin conditions (Fujii et al, 2024; Inclan-Rico et al, 2024; Liu et al, 2025). In addition to Mrgpra3+ NP2 neurons, hBD2 also activated subsets of β-alanine− or serotonin-responsive populations (NP1 and NP3 neurons), suggesting that hBD2-responsive neurons are heterogeneous.

In addition to direct neuronal activation, we also explored the possibility that defensins cause psoriatic inflammation and itch through mast cell activation. Previous studies have shown that β-defensins can trigger mast cell degranulation through the Mrgprb2 receptor (Liu et al, 2025; Shao et al, 2022; Subramanian et al, 2013; Tseng and Hoon, 2022). We used the IMQ model on the nape skin of WT and *Mrgprb2*-knockout mice and monitored erythema, scaling, cumulative psoriasis severity index, and skin thickness over time. IMQ-treated *Mrgprb2*-knockout mice did not show a significant phenotype compared with IMQ-treated WT mice (Supplementary Figure S10a–e). These data suggest that mast cells might not be the primary defensin effector cells and that other defensin signaling pathways might be involved in mediating psoriatic inflammation.

Our findings position defensins at the intersection of KC inflammation, innate immune activation, and sensory neuron excitability. However, several open questions remain. First, we are currently investigating the mechanisms through which defensins regulate neutrophil activities in psoriasis. Recent high-throughput sequencing has revealed various circulating neutrophil states and tissue specificities (Hatje et al, 2025; Nishide et al, 2025; Xie et al, 2020). Transcriptomics analysis of neutrophils isolated from IMQ-treated skin of WT and *Def* cKO mice is required to further understand the effects of defensins on neutrophil signaling and gene expression. Second, although our study solved the genetic redundancy problem using a cluster knockout approach, we could not resolve the effects of individual defensins. In addition to *Defb4* and *Defb14*, other defensins and AMP families may cooperate to sustain chronic inflammation and itch. Third, although our 16S analysis showed that IMQ treatment altered the skin microbiome in both WT and *Def* cKO mice, these data do not establish whether microbial changes contribute to the reduced inflammation or itch observed in *Def* cKO animals. Future studies using antibiotic treatment, gnotobiotic models, and microbial reconstitution will be needed to determine whether altered microbial communities contribute to inflammation and itch in psoriasis. Fourth, psoriasis involves a wide array of immune populations, including dendritic cells, γδ T cells, innate lymphoid cells, and macrophages (Kamata and Tada, 2022; Nestle et al, 2009). In our study, we showed that *Def* cKO animals had reduced expression of IL-23, which is primarily released by dendritic cells, and it will be important to determine how defensin signaling intersects with these cellular networks. Fifth, a recent study found that Mrgpra3+ neurons regulate the expansion of IL-17+ TCRγδ T cells during helminth infections (Inclan-Rico et al, 2024), and whether these neurons play a comparable role in psoriasis remains to be investigated. Finally, our findings also have implications beyond psoriasis. Dysregulated defensin expression and neutrophil activation are features of several chronic inflammatory skin conditions, including hidradenitis suppurativa (Giamarellos-Bourboulis et al, 2016) and atopic dermatitis (Chieosilapatham et al, 2017). The identification of defensins as inflammatory mediators and pruritogens suggests that modifying defensin–neuroimmune interactions could represent a therapeutic strategy for chronic itch disorders.

In conclusion, our findings establish defensins as important neuroimmune modulators in psoriasis. By activating neutrophils, promoting the IL-17 signaling axis, and directly activating pruriceptors, KC-derived defensins serve as key regulators of both inflammation and itch. These findings illuminate, to our knowledge, a previously unreported inflammatory pathway mediated by defensins and point toward new therapeutic opportunities targeting defensin-mediated pathways in psoriasis.

MATERIALS AND METHODS

Mouse lines and IMQ-induced psoriasis model

The mouse models used in this study are C57BL/6J, *Def* cKO, *Mrgpra3*^{DTA}, *Mrgpra3*^{Tdt}, *Pirt*^{Tdt}, *Pirt*^{Gcamp6s}, *Pirt*^{Salsa}, and *Nav1.8*^{Tdt}. *Def* cKO mouse was created by XD (Dong et al, 2022). C57BL/6J, *ROSA*^{Tdt}, *ROSA*^{DTA}, *ROSA*^{Salsa}, and *Nav1.8*-cre were obtained from The Jackson Laboratory. *Pirt*-cre, *ROSA*^{Gcamp6s}, and *Mrgpra3*-cre lines were obtained from Johns Hopkins University (Han et al, 2013; Kim et al, 2008; Zhang et al, 2024). Experiments were performed using Institutional Animal Care and Use Committee–approved instructions. Age- and sex-matched mice were generally used between the ages of 7 and 10 weeks in all experiments.

To induce psoriasis, age-matched (ages 7–10 weeks) mice were anesthetized with isoflurane; their nape skin was shaved on day 0, and 5% IMQ (Padagis) was applied topically to the nape and ear for 7 days. The phenotype was observed daily by taking images and measuring skin thickness. The images were scored by a blinded experimenter on a scale of 1 to 5 to calculate the psoriasis severity index for erythema and scaling. The mice were killed on day 8, and skin was extracted from them using an 8-mm biopsy punch for downstream experiments.

Behavior studies

In the nape model, WT C57BL/6J, *Def* cKO, and *Mrgpra3*^{DTA} mice (aged 7–10 weeks) were topically treated with 5% IMQ for 7 days. The mice were habituated to a scratchAID (Automatic itch detection) chamber for 3 days (15 minutes each), and scratching behaviors were recorded for 30 minutes on day 0 and day 8 in the morning. The behavioral setup consisted of a laptop connected to a Logitech webcam, and recordings were acquired using Logitech Capture software. For the cheek injections, WT and *Mrgpra3*^{DTA} mutants (aged 7–10 weeks) were habituated in a scratchAID chamber for 3 days (15 minutes per day). A total of 20 μl of mBD4, hBD-2, and hBD-3 (100 μM in PBS) or saline were directly injected into the cheeks of WT and *Mrgpra3*^{DTA} mutants, and the scratch bouts were recorded over 30 minutes. A scratching behavior was defined as a single hind paw stroking the site of injection. The total scratch bouts were counted manually, and the total scratch time was evaluated using deep learning software (Yu et al, 2022).

Flow cytometry

Skin biopsies of 8 mm were cut into small pieces and digested in 4.5 ml RPMI without fetal bovine serum, 500 μl Liberase TL (1.67 Wunsch units/ml) (Roche), and 10% DNase 1 (Sigma-Aldrich) and incubated for 1 hour and 30 minutes at 37 °C on a rotor. The samples were then passed through a 100-μm filter to generate a cell suspension, which was then centrifuged at 300*g* for 5 minutes. The cell suspension was washed with PBS and stained using a Live/Dead Fixable Aqua Dead Cell Stain Kit (Thermo Fisher Scientific) for 30 minutes. The cells were centrifuged and resuspended in FACS buffer (2% fetal bovine serum in PBS). Cells were then treated with Monocyte Blocker (BioLegend) and Fc Block (BioLegend) for 5 minutes before the antibody cocktail was added: CD45-PerCP/Cyanine 5.5 (QA17A26, BioLegend), CD11b-PE-eFluor 610 (M1/70, Invitrogen), Ly6G-Brilliant Violet 421 (1A8, BioLegend), Siglec-F-FITC (S17007L, BioLegend), CD3-FITC (17A2, BioLegend), CD4-Brilliant Violet 605 (RM4-4, BioLegend), CD8b-APC (YTS156.7.7, BioLegend), TCR γ/δ-Brilliant Violet 421 (GL3, BioLegend), and IL-17F-PE (9D3.1C8, BioLegend); the mixture was then incubated for 30 minutes in the dark at 4 °C. Cells were then passed through a 40-μm filter, and data were collected using a BD-LSR Fortessa and analyzed using FlowJo (BD Bioscience). Neutrophils were gated as live CD45+CD11b+Ly6G+′ and IL-17 T cells were gated as live CD45+CD3+TCR γ/δ+IL-17+.

Histology

Skin samples were fixed in 4% paraformaldehyde for 2 days and then in 70% ethanol overnight, embedded in paraffin, and sectioned at 10 μm. The sections were then deparaffinized and stained with H&E according to the manufacturer's instructions (Vector Laboratories). The slides were imaged using a Keyence BZ-X800 microscope (Keyence). For immunofluorescence, skin samples were fixed in 4% paraformaldehyde for 2 days, followed by 20% sucrose for 2 days and then 30% sucrose for 2 days. Then, tissues were embedded in optimal cutting temperature and sectioned at 10 μm. The slides with the tissues were baked at 65 °C for 1 hour and blocked in a blocking buffer (5% goat serum, 1% BSA, 0.2% Triton in PBS) for 1 hour. The sections were then stained with a 1:200 dilution of rabbit antimouse Ly6G (E6Z1T, Cell Signaling Technology) in antibody-blocking buffer (5% goat serum, 1% BSA) overnight at 4 °C. The next day, sections were incubated for 1 hour at room temperature with a 1:300 dilution of Alexa Fluor 488 goat antirabbit IgG (Thermo Fisher Scientific, for neutrophil staining) and then rinsed 3 times with PBS. The slides were dried and mounted with Fluoromount-G with DAPI (Invitrogen). The slides were imaged using a ZEISS Axio Imager Z2 confocal microscope, and the images were analyzed using ImageJ (Fiji) (Schindelin et al, 2012).

Hybridization chain reaction RNA FISH and BaseScope

Cryosectioned skin tissues at 10 μm were fixed by immersing slides in ice-cold 4% paraformaldehyde for 15 minutes at 4 °C, followed by a series of ethanol washes of different percentages (50, 70, and 100%). The sections were probed for *Defb14* and hybridized overnight using a Boekel Scientific RapidFISH Slide Hybridizer. Further amplification and labeling were performed according to the manufacturer's instructions (Molecular Instruments). The images were taken using a ZEISS Axio Imager Z2 confocal microscope. For BaseScope, 10 μM paraffin-embedded skin tissues were deparaffinized and probed for *Defb4* and *K16* and amplified according to the manufacturer's instructions (ACD Bio). The slides were imaged using a Keyence BZ-X800 microscope (Keyence).

RNA extraction and RT-PCR

Skin tissues were homogenized in TRIzol reagent. Then, chloroform was added in a 1:5 ratio, mixed, and centrifuged for 15 minutes at 21000*g* at 4 °C. The top layer containing RNA was transferred to a new tube, and an equal volume of 100% ethanol was added. Then, the entire solution was transferred to a Qiagen spin column, and RNA was extracted using the Qiagen RNeasy Mini Kit (Qiagen) according to the manufacturer's instructions. The RNA was quantified using a Nanodrop, and 1000 ng of RNA was used as the template to generate cDNA with the High-Capacity cDNA Reverse Transcription kit (Applied Biosystems). qPCR was performed using TaqMan Fast Advanced Master Mix (Applied Biosystems) and TaqMan probes for genes *Defb1*, *Defb2*, *Defb3*, *Defb4*, *Defb6*, *Defb14*, *Il17a*, *Il17f*, *Il11b*, *Il23*, *Cxcl2*, *S100a8*, *S100a9*, *Tnf*, and *Actb* and performed using a Quant Studio 3 RT-PCR system (Applied Biosystems). Gene expression was normalized to *Actb* using the ΔCt method.

The 16S sequencing

Skin microbiome samples were collected by swabbing the nape skin of WT and *Def* cKO mice under control and IMQ-treated conditions.

Microbial DNA was extracted from the swabs using bead beating followed by phenol-chloroform extraction. Briefly, each swab was transferred to a sterile bead-beating tube containing 0.3 g of glass beads, extraction buffer (containing 200 mM sodium chloride, 200 mM Tris, and 20 mM EDTA), 20% SDS, and phenol:chloroform:isoamyl alcohol. Swabs were pressed against the tube wall to release sample material, chilled on ice, and homogenized by bead beating for 2 minutes at 4 °C. Samples were centrifuged to separate the aqueous and organic phases, and the aqueous phase was subjected to a second phenol:chloroform:isoamyl alcohol extraction. DNA was then precipitated with isopropanol and sodium acetate at −20 °C, washed with 100% ethanol, air dried, and resuspended in 0.1× Tris-EDTA buffer. DNA concentration was measured using a NanoDrop.

Extracted DNA was submitted to SeqCenter for 16S ribosomal RNA sequencing. Libraries were prepared by amplifying the bacterial 16S ribosomal RNA gene V3−V4 region and sequenced on an Illumina platform. Raw sequencing reads were processed and analyzed using QIIME 2 (Bolyen et al, 2019).

Isolation and stimulation of bone marrow−derived neutrophils

Bone marrows were extracted from the femur and tibia of WT C57BL/6J mice, and neutrophils were isolated using the Neutrophil Isolation Kit with magnetic-activated cell sorting (Miltenyi Biotec) following the manufacturer's instructions. Neutrophil purity was validated by flow cytometry (>95%), and 10^5 cells were seeded into a 96-well plate. The cells were then stimulated with lipopolysaccharide (100 μg/ml, Sigma-Aldrich), hBD2 (10 μM, Anaspec), hBD3 (10 μM, Anaspec), and PMA (100 μg/ml, Sigma-Aldrich) for 12 hours, and their supernatants were collected and stored at −80 °C.

ELISA

To assay IL-17 release, the cell supernatants of stimulated neutrophils were analyzed using the DuoSet ELISA Kit (R&D Systems), following the manufacturer's instructions. The optical density was measured at 450 nm, with a wavelength correction at 540 nm, using a BioTek Synergy H1 microplate reader (Agilent). A standard curve was used to quantify the released IL-17.

Lactate dehydrogenase assay

Cell viability of stimulated bone marrow−derived neutrophils was assessed after 12 hours using the LDH Cytotoxicity Assay Kit II (ab65393), according to the manufacturer's instructions. Absorbance was measured at 450 nm with wavelength correction at 650 nm using a BioTek Synergy H1 microplate reader (Agilent). Percentage cell death was calculated according to the assay instructions.

DRG isolation and culture

The spinal columns of WT C57BL/6J, *Mrgpra3*^{DTA}, and *Pirt*^{Salsa} mice aged 5−6 weeks were removed and placed in RPMI medium. DRG neurons were dissected and pooled in cold DH10 medium (DMEM/F12, 10% fetal bovine serum, and 1% penicillin−streptomycin). They were then digested in 1.1 ml of Dispase/collagenase type 1 mixture (Dispase 4 U/ml [Gibco], collagenase-1 342 U/ml [Worthington CSL-1], prepared in 1X Hank's balanced salt solution without phenol red) and incubated for 30 minutes in a rotor. The neurons were then titrated around 20 times and filtered using a 70-μm filter. The neurons were then centrifuged at 500 r.p.m. for 4 minutes and resuspended in DH10 medium. They were then plated on 8 × 8 mm coverslips coated with poly-D-lysine (0.1 mg/ml) and laminin (10 μg/ml), incubated at 37 °C, and used within 20 hours for calcium imaging.

In vitro calcium imaging

Cultured DRG neurons from *Pirt*^{Salsa} mice express a genetically encoded calcium indicator GCaMP6f. DRG neurons from WT C57BL/6J and *Mrgpra3*^{DTA} were loaded with 5 μM Fluo-4 AM (Invitrogen) for 30 minutes in the dark. The neurons were then washed with calcium buffer (5 M sodium chloride, 1 M potassium chloride, 0.5M calcium chloride, 0.5M magnesium chloride, 10 mM 4-[2-hydroxyethyl]-1-piperazineethanesulfonic acid, 20 mM glucose, 1.19 mM sodium bicarbonate, and 20.5 mM sucrose, pH 7.4) and stimulated with hBD2 (10 μM), CQ (1 mM), β-alanine (5 mM), serotonin (5 μM), capsaicin (30 μM), and potassium chloride (100 mM). The fluorescence emission was detected at 488 nm, and the baseline fluorescence (F_0) was defined as the average fluorescence intensity across the first 30 seconds of each imaging session. The maximum fluorescence (F_t) was calculated as the average peak minus background fluorescence intensity within each region on interest across the entire recording. $\Delta F/F$ was then computed as $(F_t - F_0)/F_0$. Neuronal activation was defined as a ratio of $\Delta F/F \geq 50\%$. Each experiment contains 800−1000 cells and is analyzed.

DRG exposure surgery for in vivo calcium imaging

DRG exposure was performed as previously described (Zheng et al, 2022). Mice were anesthetized with intraperitoneal sodium pentobarbital (50−80 mg/kg). After deep anesthesia was reached, the animals' backs were shaved and aseptically prepared, and ophthalmic ointment (Lacrilube, Allergen Pharmaceuticals) was applied to the eyes to prevent drying. During the surgery, mice were kept on a heating pad (DC temperature controller, FHC) to maintain body temperature at 37 °C ± 0.5 °C as monitored by a rectal probe.

In vivo calcium imaging

In vivo imaging of whole lumbar 4 DRG was performed for 2 hours immediately after surgery. Images were acquired using a laser-scanning confocal microscope (Leica LSI microscope) equipped with a ×5 0.5 numerical aperture macro dry objective and a fast EM-CCD camera. Live images were acquired at 10 frames in frame-scan mode per 6−7 seconds, at depths of 0 to 70 mm below the dura with the DRG in the focal plane. Throughout imaging, body temperature was maintained at 37 °C ± 0.5 °C with a heating pad and rectal temperature monitoring. Anesthesia was maintained with 2% isoflurane and pure oxygen delivered through a nosecone. Mice were laid abdomen down on a custom-designed microscope stage. The spinal column was secured at 2 sites using clamps. Imaging was monitored during the activation of DRG neuron cell bodies by peripheral stimuli (10 μl of the stated concentration of either CQ or HBD2 delivered through a Hamilton syringe).

In vivo calcium imaging data analysis

Raw image stacks were collected, deconvolved, and imported into ImageJ (National Institutes of Health). Optical planes across sequential time points were realigned and motion corrected using the StackReg rigid-body algorithm. Activated neuron counts across mice and imaging sessions were normalized to the total number of DRG neurons. The total number was counted using the thresholding function in ImageJ software from a high-quality Z-stack image of DRG neurons at baseline. The size of the activated neurons was calculated using the area function in ImageJ.

Calcium signal amplitudes were expressed as $(F_t - F_0)/F_0$ as a function of time, that is, the ratio of the fluorescence difference $(F_t - F_0)$

to the basal value (F_0). The average fluorescence intensity in the baseline period was taken as F_0 and measured as the average pixel intensity during the first 2−5 frames of each imaging experiment. The maximum fluorescence intensity F_t was measured by calculating the average (peak − background) pixel values in a given region of interest for each image frame recorded during the whole recording period. F_t was then used to calculate $\Delta F/F$ using the formula $\Delta F/F = (F_t - F_0)/F_0$. Activation of a neuron was defined as an increase in fluorescence intensity, $\Delta F/F \geq 50\%$.

Statistical analysis

All statistical analyses were performed using Prism 10 (GraphPad). One-way and 2-way ANOVAs were used for multiple comparisons, as indicated in the figure legends. A 2-tailed unpaired Student's *t*-test was used for data with a single comparison. All data are presented as the mean ± SD. Statistical significance was assumed at $P < .05$.

ETHICS STATEMENT

All experimental animal procedures were approved by the Institutional Animal Care and Use Committee of the University of Texas at Dallas (approval code 2025-0192).

DATA AVAILABILITY STATEMENT

All data supporting the findings of this study are available from the corresponding author upon request.

ORCIDs

Xintong Dong: http://orcid.org/0000-0002-6887-8712
Xinzhong Dong: http://orcid.org/0000-0002-9750-7718

CONFLICT OF INTEREST

The authors state no conflict of interest.

ACKNOWLEDGMENTS

This work is funded by the National Psoriasis Foundation Discovery Award #1062013 and National Institutes of Health grant 1R01DK140039-01 awarded to XD. XD serves as the guarantor for the study and is responsible for addressing any postpublication concerns.

AUTHOR CONTRIBUTIONS

Conceptualization: SKB, XzD, XtD; Data Curation: SKB, QZ, JT, XtD; Formal Analysis: SKB, HY, JT, LGBF, YL, XtD; Funding Acquisition: WL, XzD, XtD; Writing − Original Draft Preparation: SKB, XtD

DECLARATION OF GENERATIVE ARTIFICIAL INTELLIGENCE (AI) OR LARGE LANGUAGE MODELS (LLMs)

The author(s) did not use AI/LLM in any part of the research process and/or manuscript preparation.

SUPPLEMENTARY MATERIAL

Supplementary material is linked to the online version of the paper at www.jidonline.org, and at https://doi.org/10.1016/j.jid.2026.08.014.

REFERENCES

Ali RS, Falconer A, Ikram M, Bissett CE, Cerio R, Quinn AG. Expression of the peptide antibiotics human beta defensin-1 and human beta defensin-2 in normal human skin. J Invest Dermatol 2001;117:106−11.

Bader M, Alenina N, Andrade-Navarro MA, Santos RA. MAS and its related G protein-coupled receptors. Mrgprs. Pharmacol Rev 2014;66:1080−105.

Biragyn A, Ruffini PA, Leifer CA, Klyushnenkova E, Shakhov A, Chertov O, et al. Toll-like receptor 4-dependent activation of dendritic cells by beta-defensin 2. Science 2002;298:1025−9.

Blauvelt A, Chiricozzi A. The immunologic role of IL-17 in psoriasis and psoriatic arthritis pathogenesis. Clin Rev Allergy Immunol 2018;55:379−90.

Bolyen E, Rideout JR, Dillon MR, Bokulich NA, Abnet CC, Al-Ghalith GA, et al. Reproducible, interactive, scalable and extensible microbiome data science using QIIME 2 [published correction appears in Nat Biotechnol 2019;37:1091]. Nat Biotechnol 2019;37:852−7.

Butmarc J, Yufit T, Carson P, Falanga V. Human beta-defensin-2 expression is increased in chronic wounds. Wound Repair Regen 2004;12:439−43.

Cai Y, Shen X, Ding C, Qi C, Li K, Li X, et al. Pivotal role of dermal IL-17-producing γδ T cells in skin inflammation [published correction appears in Immunity 2011;35:649]. Immunity 2011;35:596−610.

Castillo RL, Sidhu I, Dolgalev I, Chu T, Prystupa A, Subudhi I, et al. Spatial transcriptomics stratifies psoriatic disease severity by emergent cellular ecosystems. Sci Immunol 2023;8:eabq7991.

Cevikbas F, Lerner EA. Physiology and pathophysiology of itch. Physiol Rev 2020;100:945−82.

Chiang CC, Cheng WJ, Korinek M, Lin CY, Hwang TL. Neutrophils in psoriasis. Front Immunol 2019;10:2376.

Chieosilapatham P, Ogawa H, Niyonsaba F. Current insights into the role of human β-defensins in atopic dermatitis. Clin Exp Immunol 2017;190:155−66.

Czerwińska J, Owczarczyk-Saczonek A. The role of the neutrophilic network in the pathogenesis of psoriasis. Int J Mol Sci 2022;23:1840.

Di Cesare A, Di Meglio P, Nestle FO. The IL-23/Th17 axis in the immunopathogenesis of psoriasis. J Invest Dermatol 2009;129:1339−50.

Dong X, Limjunyawong N, Sypek EI, Wang G, Ortines RV, Youn C, et al. Keratinocyte-derived defensins activate neutrophil-specific receptors Mrgpra2a/b to prevent skin dysbiosis and bacterial infection. Immunity 2022;55:1645−62.e7.

Dyring-Andersen B, Honoré TV, Madelung A, Bzorek M, Simonsen S, Clemmensen SN, et al. Interleukin (IL)-17A and IL-22-producing neutrophils in psoriatic skin. Br J Dermatol 2017;177:e321−2.

Elewski B, Alexis AF, Lebwohl M, Stein Gold L, Pariser D, Del Rosso J, et al. Itch: an under-recognized problem in psoriasis. J Eur Acad Dermatol Venereol 2019;33:1465−76.

Ferretti S, Bonneau O, Dubois GR, Jones CE, Trifilieff A. IL-17, produced by lymphocytes and neutrophils, is necessary for lipopolysaccharide-induced airway neutrophilia: il-15 as a possible trigger. J Immunol 2003;170:2106−12.

Foster AM, Baliwag J, Chen CS, Guzman AM, Stoll SW, Gudjonsson JE, et al. IL-36 promotes myeloid cell infiltration, activation, and inflammatory activity in skin. J Immunol 2014;192:6053−61.

Fox S, Leitch AE, Duffin R, Haslett C, Rossi AG. Neutrophil apoptosis: relevance to the innate immune response and inflammatory disease. J Innate Immun 2010;2:216−27.

Froy O. Regulation of mammalian defensin expression by toll-like receptor-dependent and independent signalling pathways. Cell Microbiol 2005;7:1387−97.

Fujii K, Miyagawa R, Tanaka R, Saito M, Tanaka S, Shiratori-Hayashi M, et al. MrgprA3+ primary sensory neurons mediate acute allergic itch responses in atopic dermatitis model mice. Biol Pharm Bull 2024;47:1624−30.

Furue M, Furue K, Tsuji G, Nakahara T. Interleukin-17A and keratinocytes in psoriasis. Int J Mol Sci 2020;21:1275.

Fyhrquist N, Muirhead G, Prast-Nielsen S, Jeanmougin M, Olah P, Skoog T, et al. Microbe-host interplay in atopic dermatitis and psoriasis. Nat Commun 2019;10:4703.

Gao X, Ding J, Liao C, Xu J, Liu X, Lu W. Defensins: the natural peptide antibiotic. Adv Drug Deliv Rev 2021;179:114008.

Gariboldi S, Palazzo M, Zanobbio L, Selleri S, Sommariva M, Sfondrini L, et al. Low molecular weight hyaluronic acid increases the self-defense of skin epithelium by induction of beta-defensin 2 via TLR2 and TLR4. J Immunol 2008;181:2103−10.

Ghoreschi K, Balato A, Enerbäck C, Sabat R. Therapeutics targeting the IL-23 and IL-17 pathway in psoriasis. Lancet 2021;397:754−66.

Giamarellos-Bourboulis EJ, Platzer M, Karagiannidis I, Kanni T, Nikolakis G, Ulrich J, et al. High copy numbers of β-defensin cluster on 8p23.1, confer genetic susceptibility, and modulate the physical course of hidradenitis suppurativa/acne inversa. J Invest Dermatol 2016;136:1592−8.

Griffiths CEM, Armstrong AW, Gudjonsson JE, Barker JNWN. Psoriasis. Lancet 2021;397:1301−15.

Grogan MD, Bartow-McKenney C, Flowers L, Knight SAB, Uberoi A, Grice EA. Research techniques made simple: profiling the skin microbiota. J Invest Dermatol 2019;139:747−52.e1.

Guo C, Jiang H, Huang CC, Li F, Olson W, Yang W, et al. Pain and itch coding mechanisms of polymodal sensory neurons. Cell Rep 2023;42:113316.

Han L, Ma C, Liu Q, Weng HJ, Cui Y, Tang Z, et al. A subpopulation of nociceptors specifically linked to itch. Nat Neurosci 2013;16:174–82.

Hänel KH, Cornelissen C, Lüscher B, Baron JM. Cytokines and the skin barrier. Int J Mol Sci 2013;14:6720–45.

Harder J, Bartels J, Christophers E, Schröder JM. A peptide antibiotic from human skin. Nature 1997;387:861.

Harder J, Bartels J, Christophers E, Schroder JM. Isolation and characterization of human beta -defensin-3, a novel human inducible peptide antibiotic. J Biol Chem 2001;276:5707–13.

Harder J, Schröder JM. Psoriatic scales: a promising source for the isolation of human skin-derived antimicrobial proteins. J Leukoc Biol 2005;77:476–86.

Hatje K, Schneider K, Danilin S, Koechl F, Giroud N, Juglair L, et al. Comparison of single-cell RNA-seq methods to enable transcriptome profiling of neutrophils in clinical samples. Cell Rep Methods 2025;5:101173.

Hermosilla C, Caro TM, Silva LM, Ruiz A, Taubert A. The intriguing host innate immune response: novel anti-parasitic defence by neutrophil extracellular traps. Parasitology 2014;141:1489–98.

Hollox EJ, Huffmeier U, Zeeuwen PL, Palla R, Lascorz J, Rodijk-Olthuis D, et al. Psoriasis is associated with increased beta-defensin genomic copy number. Nat Genet 2008;40:23–5.

Hu P, Wang M, Gao H, Zheng A, Li J, Mu D, et al. The role of helper T cells in psoriasis. Front Immunol 2021;12:788940.

Hu S, He W, Du X, Yang J, Wen Q, Zhong XP, et al. IL-17 production of neutrophils enhances antibacteria ability but promotes arthritis development during Mycobacterium tuberculosis infection. EBiomedicine 2017;23:88–99.

Inclan-Rico JM, Napuri CM, Lin C, Hung LY, Ferguson AA, Liu X, et al. MrgprA3 neurons drive cutaneous immunity against helminths through selective control of myeloid-derived IL-33. Nat Immunol 2024;25:2068–84.

Inozemtsev V, Sergunova V, Vorobjeva N, Kozlova E, Sherstyukova E, Lyapunova S, et al. Stages of NETosis development upon stimulation of neutrophils with activators of different types. Int J Mol Sci 2023;24:12355.

Jansen PAM, Rodijk-Olthuis D, Hollox EJ, Kamsteeg M, Tjabringa GS, de Jongh GJ de, et al. β-defensin-2 protein is a serum biomarker for disease activity in psoriasis and reaches biologically relevant concentrations in lesional skin. PLoS One 2009;4:e4725.

Kamata M, Tada Y. Dendritic cells and macrophages in the pathogenesis of psoriasis. Front Immunol 2022;13:941071.

Kamiya K, Kishimoto M, Sugai J, Komine M, Ohtsuki M. Risk factors for the development of psoriasis. Int J Mol Sci 2019;20:4347.

Kienle K, Lämmermann T. Neutrophil swarming: an essential process of the neutrophil tissue response. Immunol Rev 2016;273:76–93.

Kim AY, Tang Z, Liu Q, Patel KN, Maag D, Geng Y, et al. Pirt, a phosphoinositide-binding protein, functions as a regulatory subunit of TRPV1. Cell 2008;133:475–85.

Kim J, Lee J, Kim HJ, Kameyama N, Nazarian R, Der E, et al. Single-cell transcriptomics applied to emigrating cells from psoriasis elucidate pathogenic versus regulatory immune cell subsets. J Allergy Clin Immunol 2021;148:1281–92.

Kolar SS, Baidouri H, Hanlon S, McDermott AM. Protective role of murine β-defensins 3 and 4 and cathelin-related antimicrobial peptide in Fusarium solani keratitis. Infect Immun 2013;81:2669–77.

Kolbinger F, Loesche C, Valentin MA, Jiang X, Cheng Y, Jarvis P, et al. β-Defensin 2 is a responsive biomarker of IL-17A–driven skin pathology in patients with psoriasis. J Allergy Clin Immunol 2017;139:923–32.e8.

Komiya E, Tominaga M, Kamata Y, Suga Y, Takamori K. Molecular and cellular mechanisms of itch in psoriasis. Int J Mol Sci 2020;21:8406.

Kumar A, Zhang J, Yu FS. Toll-like receptor 2-mediated expression of beta-defensin-2 in human corneal epithelial cells. Microbes Infect 2006;8:380–9.

Kusuba N, Kitoh A, Dainichi T, Honda T, Otsuka A, Egawa G, et al. Inhibition of IL-17-committed T cells in a murine psoriasis model by a vitamin D analogue. J Allergy Clin Immunol 2018;141:972–81.e10.

Langley RG, Krueger GG, Griffiths CE. Psoriasis: epidemiology, clinical features, and quality of life. Ann Rheum Dis 2005;64(Suppl 2):ii18–23 [discussion ii24].

Li L, Huang L, Vergis AL, Ye H, Bajwa A, Narayan V, et al. IL-17 produced by neutrophils regulates IFN-gamma-mediated neutrophil migration in mouse kidney ischemia-reperfusion injury. J Clin Invest 2010;120:331–42.

Lin AM, Rubin CJ, Khandpur R, Wang JY, Riblett M, Yalavarthi S, et al. Mast cells and neutrophils release IL-17 through extracellular trap formation in psoriasis. J Immunol 2011;187:490–500.

Lin L, Luo Q, Gao X, Li Q, Li W, Zhou X, et al. Correlation and clinical significance of HBD-2 and CXCL-1/2 levels at skin lesions with psoriasis vulgaris severity. Immunol Invest 2024;53:1234–49.

Liu AW, Zhang YR, Chen CS, Edwards TN, Ozyaman S, Ramcke T, et al. Scratching promotes allergic inflammation and host defense via neurogenic mast cell activation. Science 2025;387:eadn9390.

Liu Q, Sikand P, Ma C, Tang Z, Han L, Li Z, et al. Mechanisms of itch evoked by β-alanine. J Neurosci 2012;32:14532–7.

Liu Q, Tang Z, Surdenikova L, Kim S, Patel KN, Kim A, et al. Sensory neuron-specific GPCR Mrgprs are itch receptors mediating chloroquine-induced pruritus. Cell 2009;139:1353–65.

Man AM, Orăsan MS, Hoteiuc OA, Olănescu-Vaida-Voevod MC, Mocan T. Inflammation and psoriasis: a comprehensive review. Int J Mol Sci 2023;24:16095.

Martin DA, Towne JE, Kricorian G, Klekotka P, Gudjonsson JE, Krueger JG, et al. The emerging role of IL-17 in the pathogenesis of psoriasis: preclinical and clinical findings. J Invest Dermatol 2013;133:17–26.

McGill CJ, Lu RJ, Benayoun BA. Protocol for analysis of mouse neutrophil NETosis by flow cytometry. STAR Protoc 2021;2:100948.

McNeil B, Dong X. Mrgprs as itch receptors. In: Carstens E, Akiyama T, editors. Itch: mechanisms and treatment. Boca Raton: CRC Press/Taylor and Francis; 2014.

Meixiong J, Anderson M, Limjunyawong N, Sabbagh MF, Hu E, Mack MR, et al. Activation of mast-cell-expressed mas-related G-protein-coupled receptors drives non-histaminergic itch. Immunity 2019;50:1163–71.e5.

Meixiong J, Dong X. Mas-related G protein-coupled receptors and the biology of itch sensation. Annu Rev Genet 2017;51:103–21.

Merleev A, Ji-Xu A, Toussi A, Tsoi LC, Le ST, Luxardi G, et al. Proprotein convertase subtilisin/kexin type 9 is a psoriasis-susceptibility locus that is negatively related to IL36G. JCI Insight 2022;7:e141193.

Morizane S, Gallo RL. Antimicrobial peptides in the pathogenesis of psoriasis. J Dermatol 2012;39:225–30.

Morrison G, Kilanowski F, Davidson D, Dorin J. Characterization of the mouse beta defensin 1, Defb1, mutant mouse model. Infect Immun 2002;70:3053–60.

Mosca M, Hong J, Hadeler E, Hakimi M, Liao W, Bhutani T. The role of IL-17 cytokines in psoriasis. ImmunoTargets Ther 2021;10:409–18.

Navid F, Boniotto M, Walker C, Ahrens K, Proksch E, Sparwasser T, et al. Induction of regulatory T cells by a murine β-defensin. J Immunol 2012;188:735–43.

Nestle FO, Kaplan DH, Barker J. Psoriasis. N Engl J Med 2009;361:496–509.

Nishide M, Nishimura K, Matsushita H, Kawada S, Shimagami H, Metsugi S, et al. Neutrophil single-cell analysis identifies a type II interferon-related subset for predicting relapse of autoimmune small vessel vasculitis. Nat Commun 2025;16:3581.

Nussbaum L, Chen YL, Ogg GS. Role of regulatory T cells in psoriasis pathogenesis and treatment. Br J Dermatol 2021;184:14–24.

Orsmond A, Bereza-Malcolm L, Lynch T, March L, Xue M. Skin barrier dysregulation in psoriasis. Int J Mol Sci 2021;22:10841.

Petit RG, Cano A, Ortiz A, Espina M, Prat J, Muñoz M, et al. Psoriasis: from pathogenesis to pharmacological and nano-technological-based therapeutics. Int J Mol Sci 2021;22:4983.

Potestio L, Martora F, Lauletta G, Vallone Y, Battista T, Megna M. The role of interleukin 23/17 axis in psoriasis management: a comprehensive review of clinical trials. Clin Cosmet Investig Dermatol 2024;17:829–42.

Qi C, Wang Y, Li P, Zhao J. Gamma Delta T Cells and their pathogenic role in psoriasis. Front Immunol 2021;12:627139.

Radic M, Marion TN. Neutrophil extracellular chromatin traps connect innate immune response to autoimmunity. Semin Immunopathol 2013;35:465–80.

Reich A, Szepietowski JC. Mediators of pruritus in psoriasis. Mediators Inflamm 2007;2007:64727.

Saito-Sasaki N, Sawada Y. S100 proteins in the pathogenesis of psoriasis and atopic dermatitis. Diagnostics (Basel) 2023;13:3167.

Sakai K, Sanders KM, Youssef MR, Yanushefski KM, Jensen L, Yosipovitch G, et al. Mouse model of imiquimod-induced psoriatic itch. Pain 2016;157:2536–43.

Sato Y, Ogawa E, Okuyama R. Role of innate immune cells in psoriasis. Int J Mol Sci 2020;21:6604.

Schindelin J, Arganda-Carreras I, Frise E, Kaynig V, Longair M, Pietzsch T, et al. Fiji: an open-source platform for biological-image analysis. Nat Methods 2012;9:676–82.

Semple F, Dorin JR. β-Defensins: multifunctional Modulators of Infection, Inflammation and More? J Innate Immun 2012;4:337–48.

Shao M, Yuan F, Liu J, Luo H. Mast cell specific receptor Mrgprb2 regulating experimental colitis is associated with the microbiota-gut-brain axis. J Inflamm Res 2022;15:6137–51.

Shelley JR, Davidson DJ, Dorin JR. The dichotomous responses driven by β-defensins. Front Immunol 2020;11:1176.

Sieminska I, Pieniawska M, Grzywa TM. The immunology of psoriasis-current concepts in pathogenesis. Clin Rev Allergy Immunol 2024;66:164–91.

Štrajtenberger M, Stipić-Marković A, Barac E, Artuković M, Lugović-Mihić L. Human β-defensin 2: a connection between infections and allergic skin diseases. Acta Dermatovenerol Alp Pannonica Adriat 2024;33:135–9.

Subramanian H, Gupta K, Lee D, Bayir AK, Ahn H, Ali H. β-defensins activate human mast cells via mas-related gene X2. J Immunol 2013;191:345–52.

Sumikawa Y, Asada H, Hoshino K, Azukizawa H, Katayama I, Akira S, et al. Induction of beta-defensin 3 in keratinocytes stimulated by bacterial lipopeptides through toll-like receptor 2. Microbes Infect 2006;8:1513–21.

Taliercio VL, Snyder AM, Webber LB, Langner AU, Rich BE, Beshay AP, et al. The disruptiveness of itchiness from psoriasis: a qualitative study of the impact of a single symptom on quality of life. J Clin Aesthet Dermatol 2021;14:42–8.

Tian S, Chen S, Feng Y, Li Y. The interactions of small proline-rich proteins with late cornified envelope proteins are involved in the pathogenesis of psoriasis. Clin Cosmet Investig Dermatol 2021;14:1355–65.

Tseng PY, Hoon MA. Specific β-defensins stimulate pruritus through activation of sensory neurons. J Invest Dermatol 2022;142:594–602.

Tsoi LC, Rodriguez E, Degenhardt F, Baurecht H, Wehkamp U, Volks N, et al. Atopic dermatitis is an IL-13-dominant disease with greater molecular heterogeneity compared to psoriasis. J Invest Dermatol 2019;139:1480–9.

van der Fits L, Mourits S, Voerman JS, Kant M, Boon L, Laman JD, et al. Imiquimod-induced psoriasis-like skin inflammation in mice is mediated via the IL-23/IL-17 axis. J Immunol 2009;182:5836–45.

Vijayapoopathi S, Ramamoorthy R, Meganathan J, Kalaiyazhagan A, Bhuvarahamurthy S, Venugopal B. Nutraceutical combination ameliorates imiquimod-induced psoriasis in mice. Chem Biol Drug Des 2023;102:1578–87.

Vora P, Youdim A, Thomas LS, Fukata M, Tesfay SY, Lukasek K, et al. Beta-Defensin-2 expression is regulated by TLR signaling in intestinal epithelial cells. J Immunol 2004;173:5398–405.

Wang WM, Jin HZ. Role of neutrophils in psoriasis. J Immunol Res 2020;2020:3709749.

Wang X, Sun J, Hu J. IMQ induced K14-VEGF mouse: a stable and long-term mouse model of psoriasis-like inflammation. PLoS One 2015;10:e0145498.

Wang Z, Shi D. Research progress on the neutrophil components and their interactions with immune cells in the development of psoriasis. Skin Res Technol 2023;29:e13404.

Xie X, Shi Q, Wu P, Zhang X, Kambara H, Su J, et al. Single-cell transcriptome profiling reveals neutrophil heterogeneity in homeostasis and infection. Nat Immunol 2020;21:1119–33.

Xu D, Lu W. Defensins: a double-edged sword in host immunity. Front Immunol 2020;11:764.

Yang D, Chertov O, Bykovskaia SN, Chen Q, Buffo MJ, Shogan J, et al. β-Defensins: linking Innate and Adaptive Immunity through dendritic and T cell CCR6. Science 1999;286:525–8.

Yosipovitch G, Rosen JD, Hashimoto T. Itch: from mechanism to (novel) therapeutic approaches. J Allergy Clin Immunol 2018;142:1375–90.

Yu H, Xiong J, Ye AY, Cranfill SL, Cannonier T, Gautam M, et al. Scratch-AID, a deep learning-based system for automatic detection of mouse scratching behavior with high accuracy. Elife 2022;11:e84042.

Zhang C, Huang Q, Ford NC, Limjunyawong N, Lin Q, Yang F, et al. Human birth tissue products as a non-opioid medicine to inhibit post-surgical pain. ELife 2024;13:RP101269.

Zhang J, Yu Q, Qu Y, Tan J, Dai Q, Jia Y, et al. Mrgpra2+ neutrophils integrate infection-derived signals to trigger NET-mediated antimicrobial defense in bone marrow. Cell Rep 2026;45:117579.

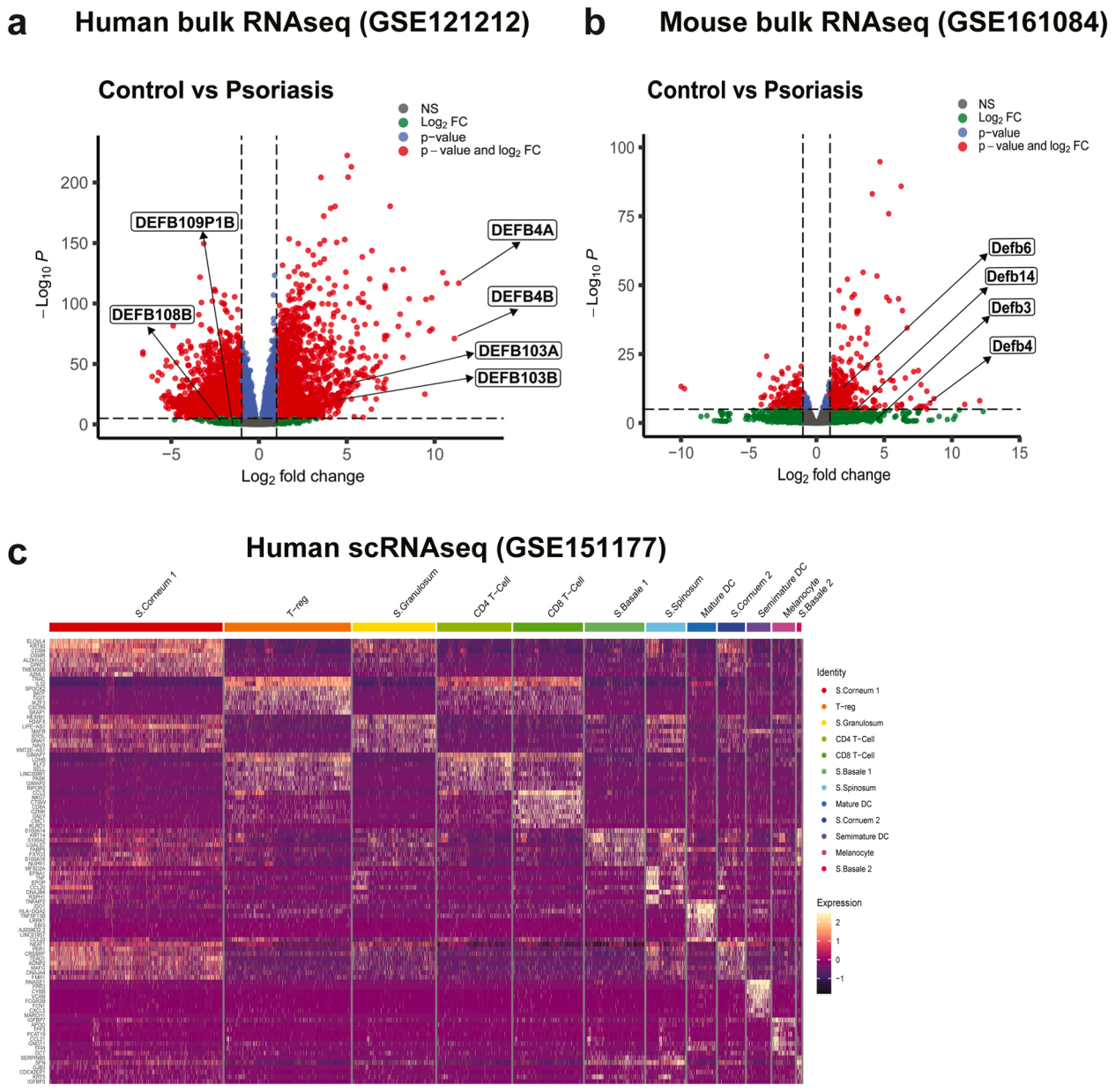
Zhang L, McNeil BD. Beta-defensins are proinflammatory pruritogens that activate Mrgprs. J Allergy Clin Immunol 2019;143:1960–2.e5.

Zhang Q, Jang M, Dias FC, Zeng Q, Wang P, Tai H, et al. Neuronal mechanisms of psoriatic itch: role of IL-17R/ERK/TRPV4 signaling pathway. J Invest Dermatol 2025;145:2753–62.e3.

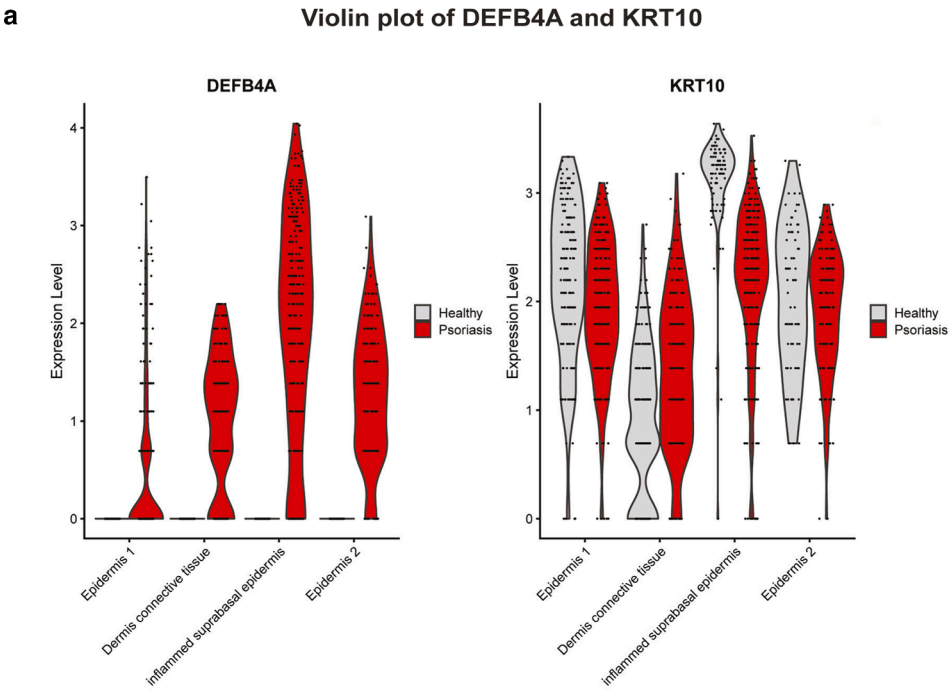
Zhang X, Li X, Chen Y, Li B, Guo C, Xu P, et al. Xiao-Yin-Fang therapy alleviates psoriasis-like skin inflammation through suppressing γδT17 cell polarization. Front Pharmacol 2021;12:629513.

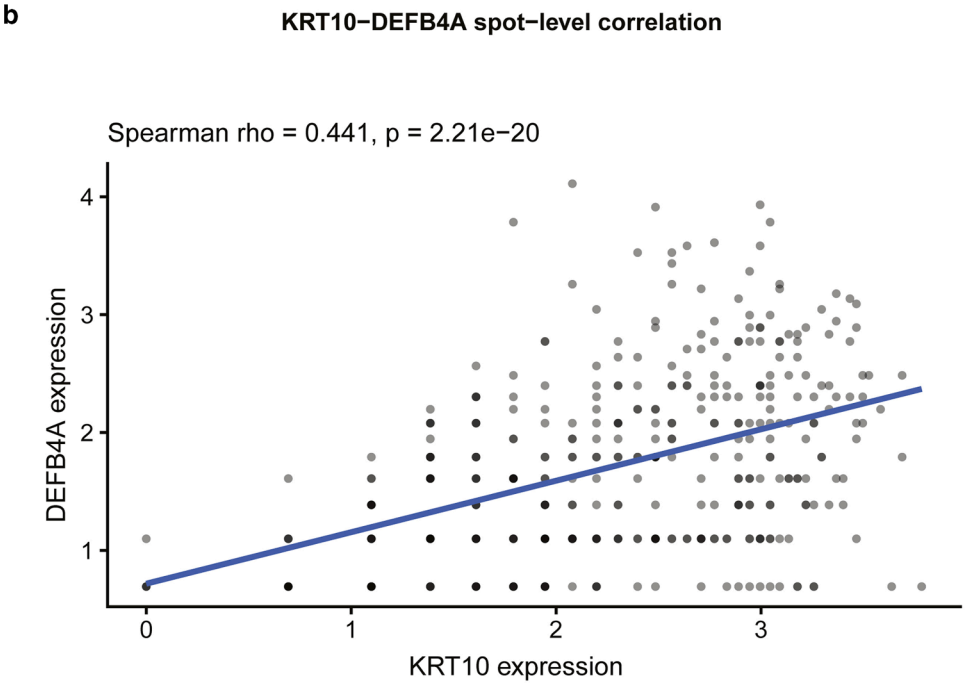
Zheng Q, Xie W, Lückemeyer DD, Lay M, Wang XW, Dong X, et al. Synchronized cluster firing, a distinct form of sensory neuron activation, drives spontaneous pain. Neuron 2022;110:209–20.e6.

Zhou YS, Webb S, Lettice L, Tardif S, Kilanowski F, Tyrrell C, et al. Partial deletion of chromosome 8 β-defensin cluster confers sperm dysfunction and infertility in male mice. PLoS Genet 2013;9:e1003826.

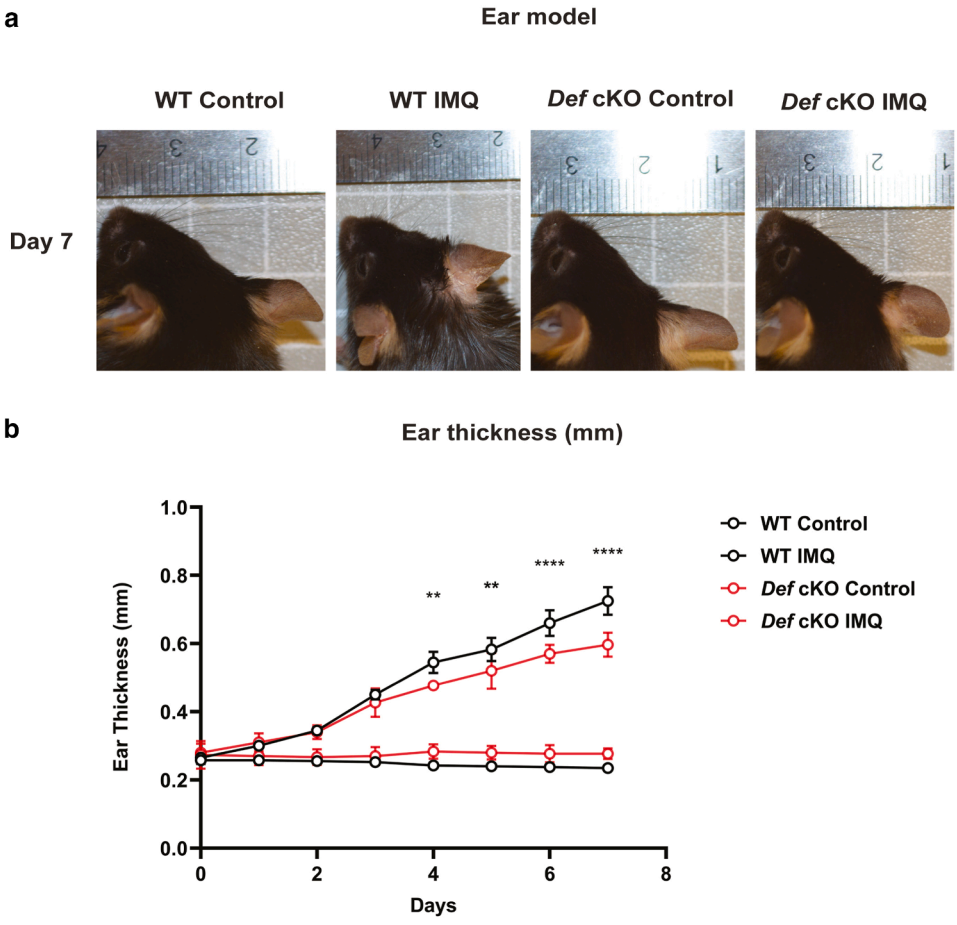


Supplementary Figure S1. Defensin expression is elevated in human and mouse psoriatic tissues. (**a**) Volcano plot showing the differentially expressed genes (*DEFB4A* and *DEFB103B*) in human lesional psoriatic skin compared with those in control skin (GSE 121212). (**b**) Bulk RNA-sequencing analysis of IMQ-treated mouse skin (GSE161084). Volcano plot shows the differentially expressed genes (*Defb4*, *Defb3*, *Defb6*, and *Defb14*) in IMQ-treated skin compared with those in control skin. (**c**) Analysis of published human scRNA-seq data (GSE151177). Heatmap shows the top 8 differentially expressed genes in each subcluster; purple indicates low expression; orange indicates high expression. IMQ, imiquimod; scRNA-seq, single-cell RNA sequencing.

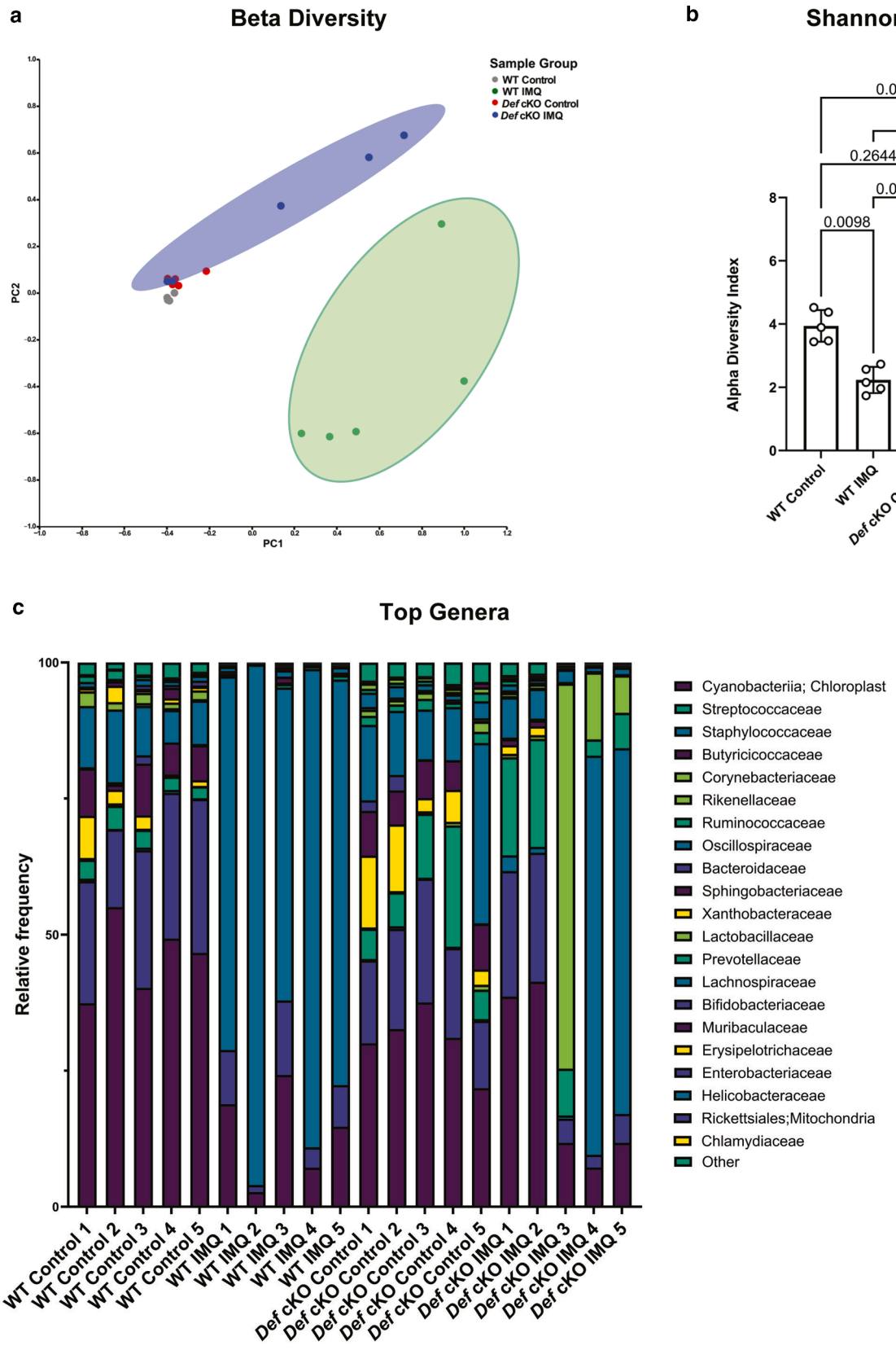




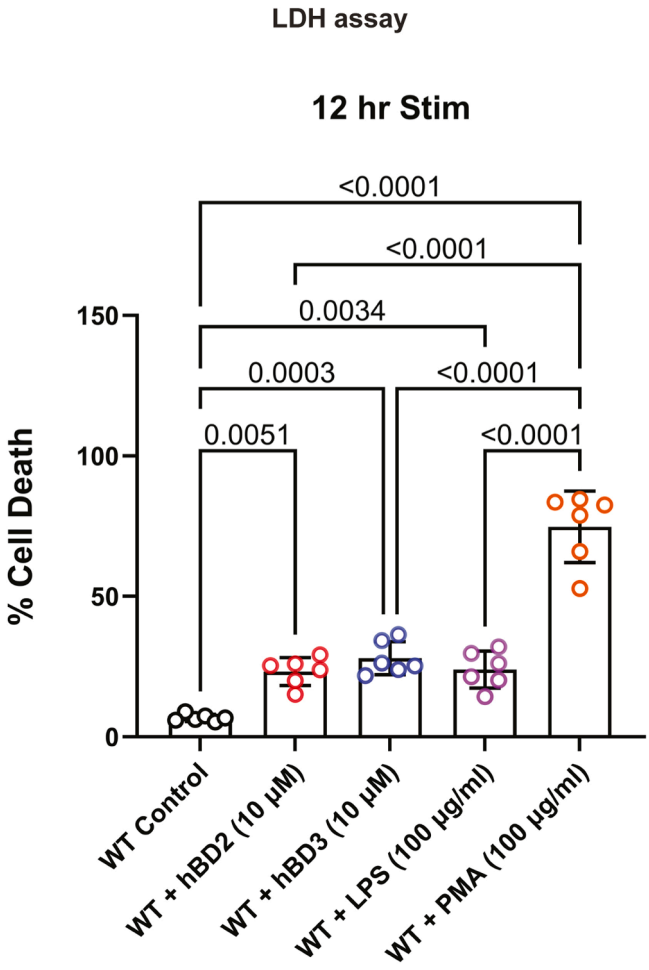
Supplementary Figure S2. Spatial transcriptomic analysis of DEFB4A and K10 expression in psoriatic skin. (**a**) Violin plots showing normalized *DEFB4A* and *K10* expression across annotated spatial clusters (epidermis 1, dermis connective tissue, inflamed suprabasal epidermis, and epidermis 2) in healthy and psoriatic skin. *DEFB4A* expression is highest in the inflamed suprabasal epidermis, whereas *K10* is broadly expressed in all 4 clusters. (**b**) Spot-level correlation analysis between *DEFB4A* and *K10* expression across *DEFB4A*+ subclustered spatial transcriptomic spots. Spearman's rho = 0.441, $P = 2.21 \times 10^{-20}$.



Supplementary Figure S3. IMQ-treated Def cKO animals show reduced psoriatic inflammation in the ear model. (**a**) Representative images of ears from control and IMQ-treated WT and *Def* cKO mice on day 7 of the ear psoriasis-like inflammation model. (**b**) Quantification of ear thickness over 7 days of IMQ treatment (n = 3–4). Data are presented as mean ± SD. $^{**}P < .01$ and $^{****}P < .0001$. Two-way ANOVA and Tukey's multiple comparison test were used to calculate the *P*-values. IMQ, imiquimod; WT, wild-type.

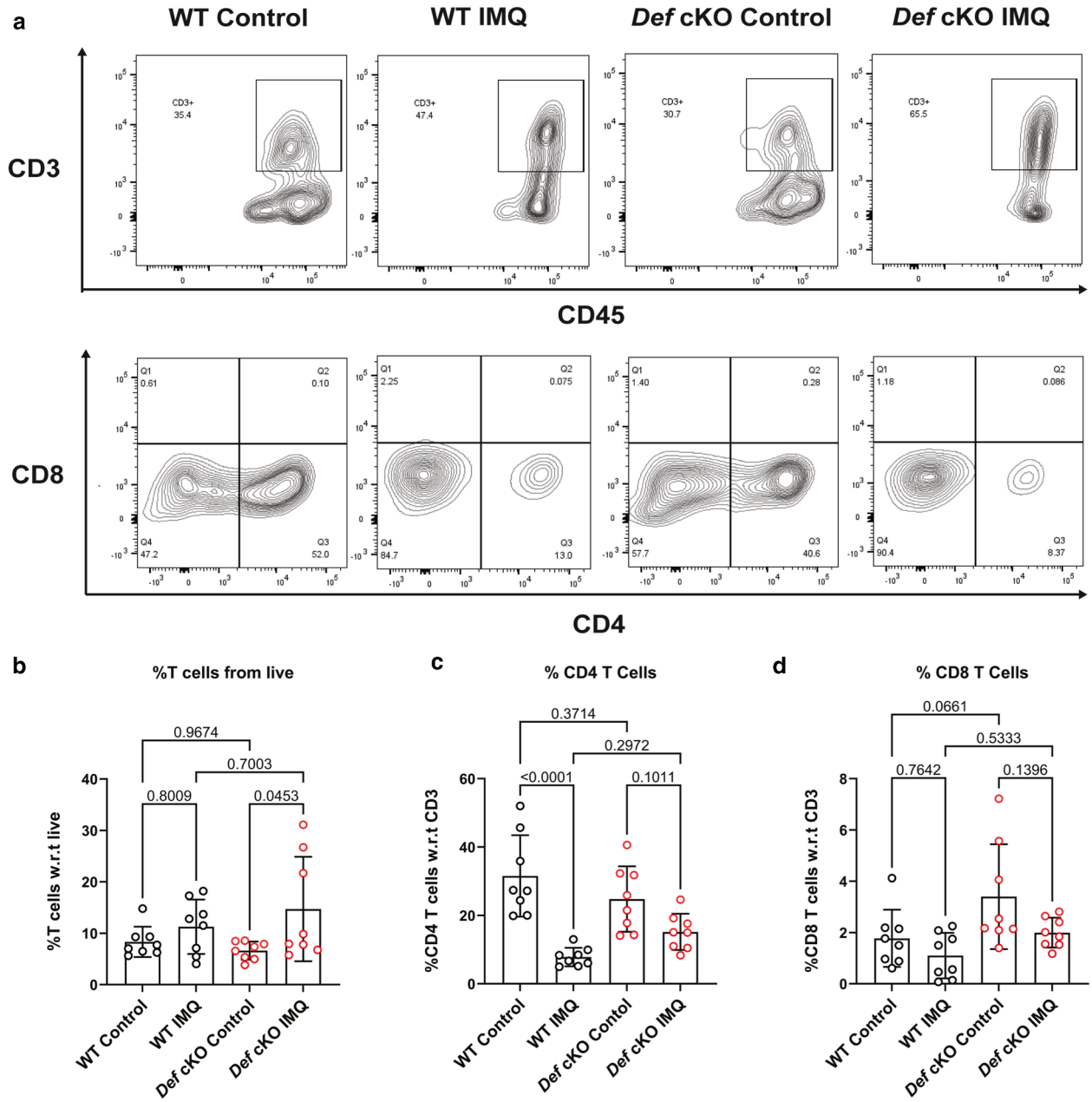


Supplementary Figure S4. IMQ treatment alters the skin microbiome in WT and Def cKO mice. (**a**) Beta diversity analysis of 16S rRNA sequencing data from nape skin swabs collected from control and IMQ-treated WT and *Def* cKO mice. Principal coordinate analysis shows that WT control (gray) and *Def* cKO (red) control samples cluster closely together, whereas IMQ-treated WT (green) and *Def* cKO (purple) form distinct clusters. Each point represents an individual mouse sample. (**b**) Shannon alpha diversity index of skin microbiome samples from the control and IMQ-treated WT and *Def* cKO mice (n = 5). (**c**) Stacked bar

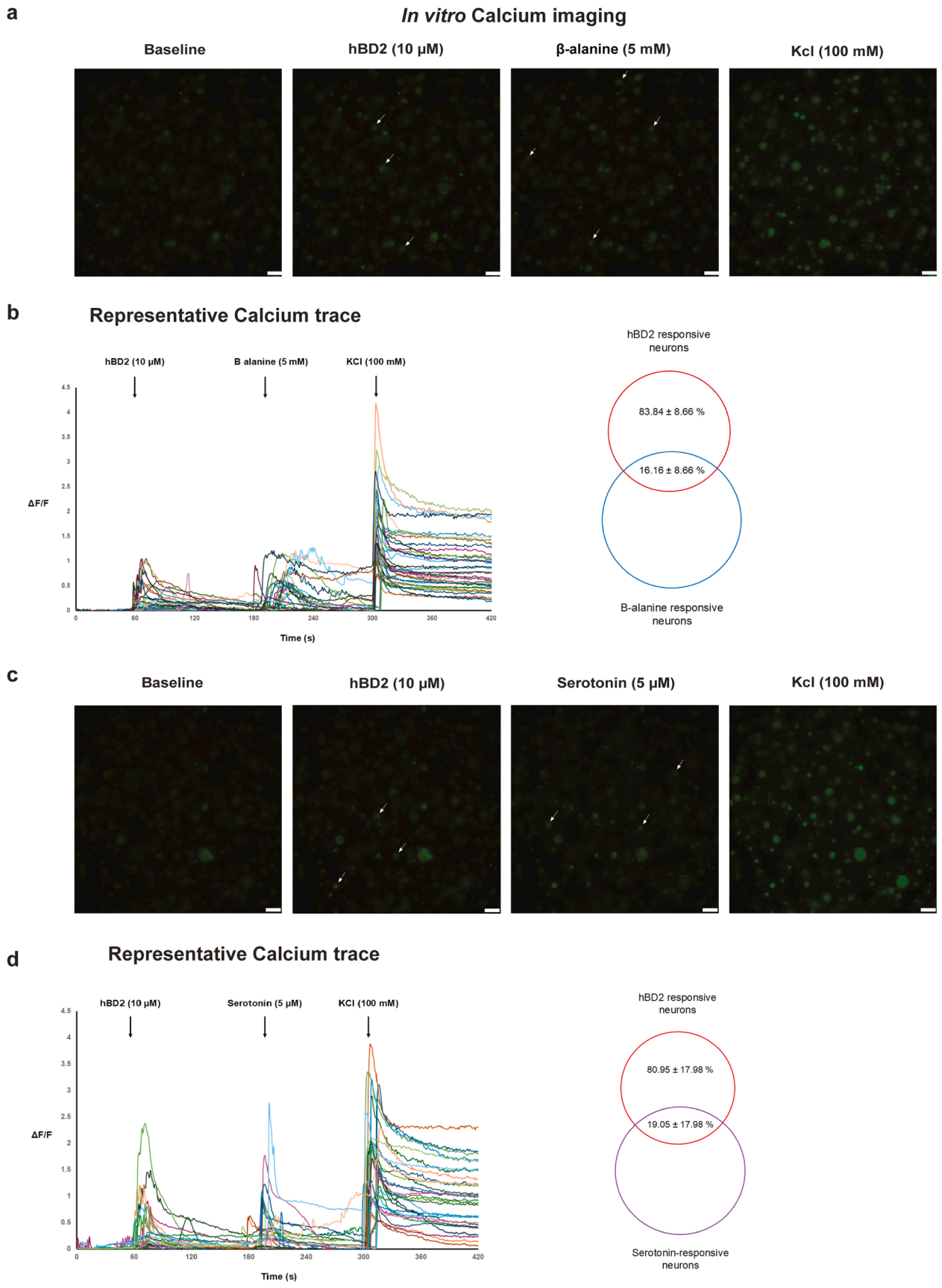


Supplementary Figure S5. Defensin stimulation does not induce significant cell death in bone marrow–derived neutrophils. LDH cytotoxicity assay of WT bone marrow–derived neutrophils after 12 hours of stimulation with hBD2 (10 μM), hBD3 (10 μM), LPS (100 μg/ml), and PMA (100 μg/ml). Percentage cell death was quantified from LDH release in the culture supernatant. Data are presented as mean ± SD. One-way ANOVA was used to calculate the *P*-values. hBD2, human β-defensin 2; hBD3, human β-defensin 3; LDH, lactate dehydrogenase; PMA, phorbol 12-myristate 13-acetate; WT, wild-type.

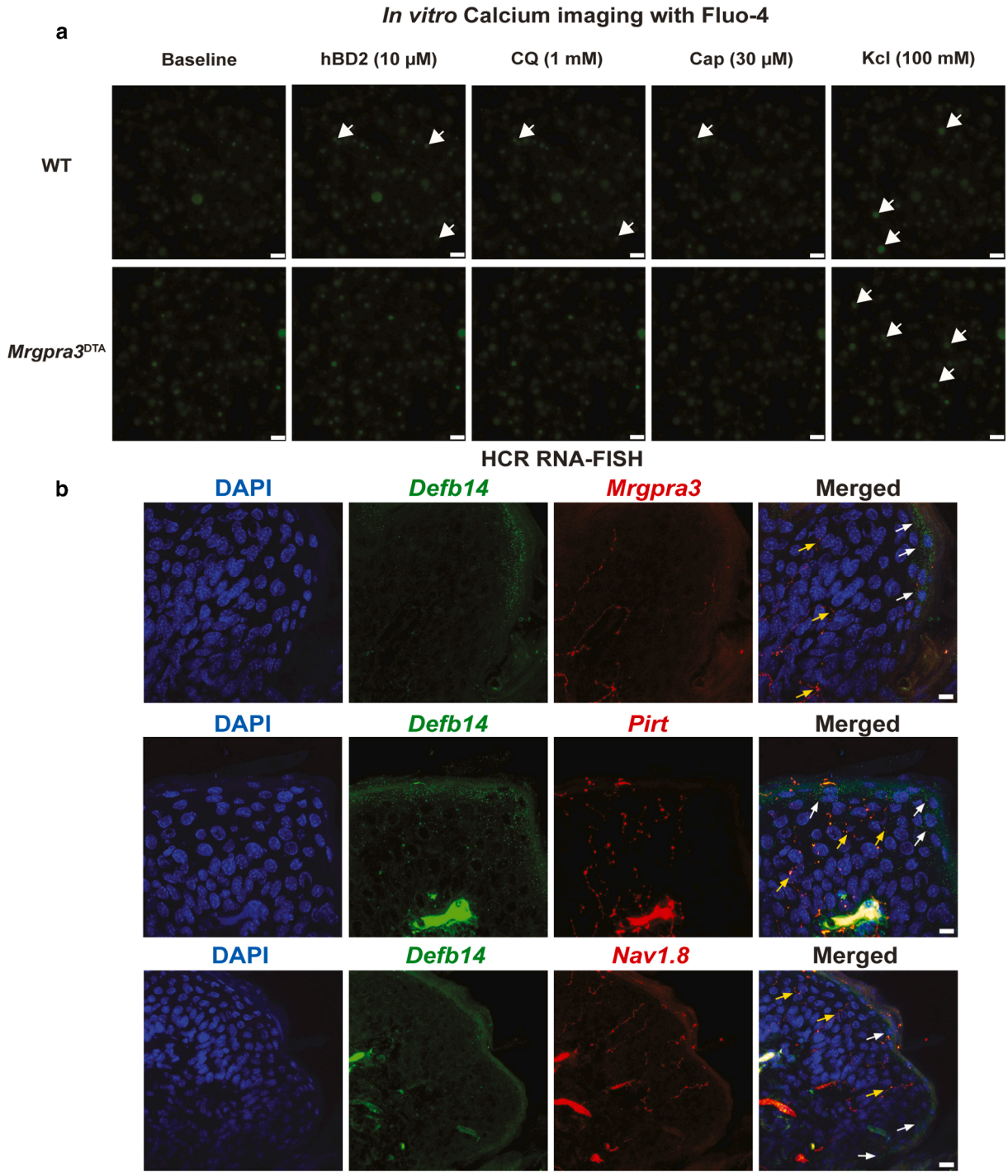
charts depicting the relative abundance of the top bacterial genera detected by 16S rRNA sequencing across control and IMQ-treated WT and *Def* cKO skin samples. Data are presented as mean ± SD. One-way ANOVA was used to calculate the *P*-values. IMQ, imiquimod; rRNA, ribosomal RNA; WT, wild-type.



Supplementary Figure S6. Defensin does not affect the overall T-cell populations in IMQ-induced psoriasis. (**a**) Flow cytometric analysis of T-cell subsets in WT and *Def* cKO skin after 7 days of IMQ treatment. The gating strategy is shown for $CD45^{+}CD3^{+}$ total T cells, followed by $CD4^{+}$ and $CD8^{+}$ T cells. (**b**) Quantification of total $CD3^{+}$ T cells with respect to live in WT and *Def* cKO IMQ-treated skin (n = 8). (**c, d**) Quantification of $CD4^{+}$ T cells and $CD8^{+}$ T cells with respect to CD3 in WT and *Def* cKO IMQ-treated skin (n = 8). Data are presented as mean ± SD. One-way ANOVA was used to calculate the *P*-values. IMQ, imiquimod; WT, wild-type.

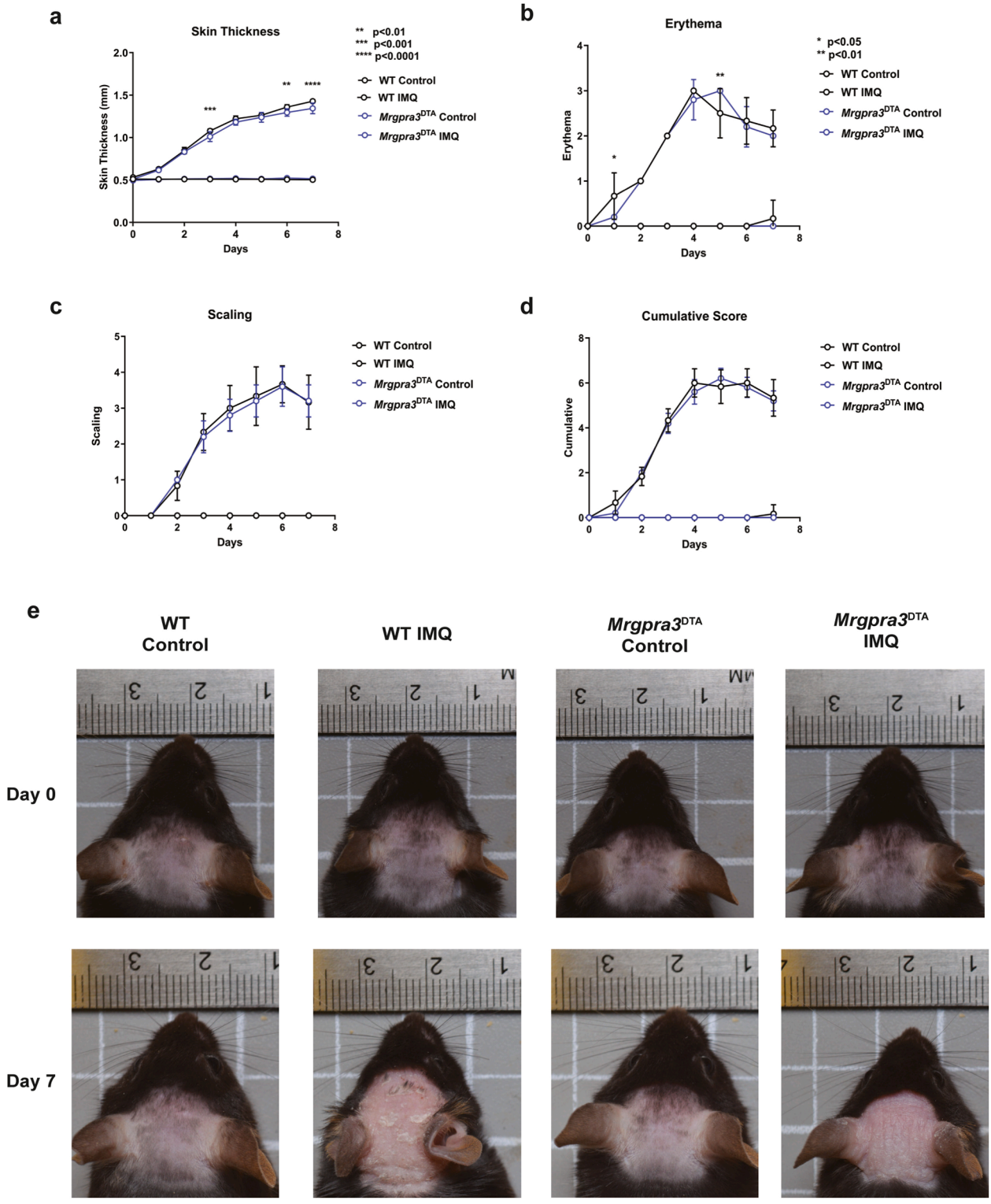


Supplementary Figure S7. Defensin-responsive neurons show limited overlap with β-alanine– and serotonin-responsive neuronal populations. (**a**) In vitro calcium images of cultured DRG neurons from WT mice. The neurons are labeled with Fluo-4 for 30 minutes and stimulated with hBD2 (10 μM), β-alanine (5 mM), and KCl (100 mM). Bar = 50 μm (n = 3). (**b**) Representative calcium trace of hBD2, β-alanine, and KCl is shown. Arrows point at the neurons activated by

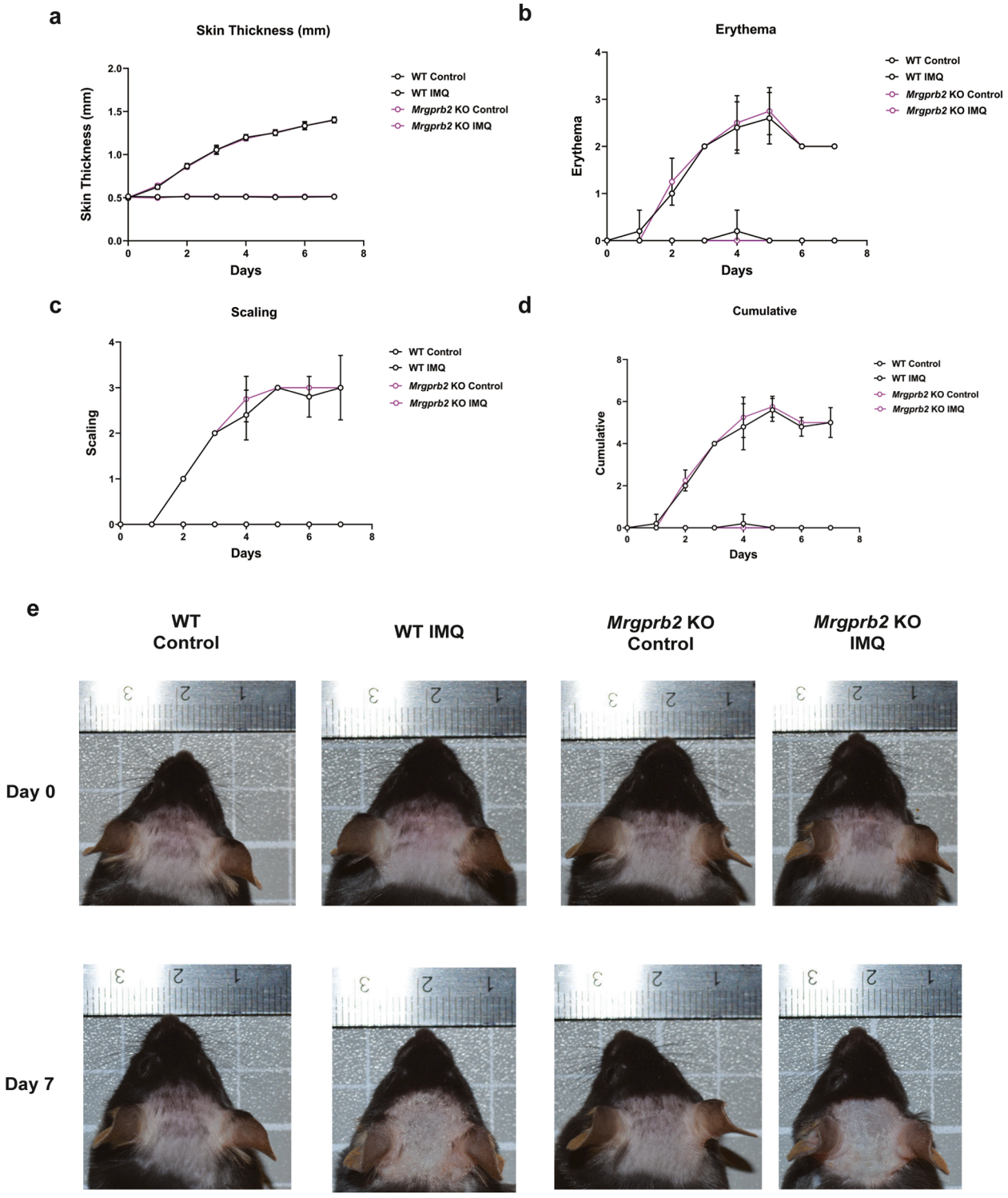


Supplementary Figure S8. Defensins activate Mrgpra3 neurons and colocalize near the Mrgpra3 nerve terminals in psoriatic skin. (**a**) Representative in vitro calcium images of cultured DRG neurons from WT and *Mrgpra3*^{DTA} mice loaded with calcium indicator Fluo-4. The neurons are stimulated with hBD2 (10 μM), CQ (1 mM), capsaicin (cap) (30 μM), and KCl (100 mM). Arrows point at the neurons activated by hBD2, CQ, and cap. Bar = 50 μm (n = 5). (**b**) Representative HCR RNA FISH images of *Defb*14 transcripts (green puncta) in IMQ-treated *Mrgpra3*^{Tdtomato}, *Pirt*^{Tdtomato}, and *Nav1.8*^{Tdtomato}, in which the Mrgpra3, Pirt, and Nav1.8 neurons express Tdtomato. Neurons are shown in red, and nuclei are labeled with DAPI (n = 3). Bar = 50 μm. CQ, chloroquine; DRG, dorsal root ganglion; hBD2, human β-defensin 2; HCR, hybridization chain reaction; IMQ, imiquimod; KCl, potassium chloride; WT, wild-type.

hBD2 and β-alanine. ΔF/F cutoff for activation is 0.5. Venn diagram shows that among hBD2-activated neurons, 16.16 ± 8.66% responded to β-alanine. (**c**) In vitro calcium images of cultured DRG neurons from WT mice. The neurons are labeled with Fluo-4 for 30 minutes and stimulated with hBD2 (10 μM), serotonin (5 μM), and KCl (100 mM). Bar = 50 μm (n = 3). (**d**) Representative calcium trace of hBD2, serotonin, and KCl. Arrows point at the neurons activated by hBD2 and serotonin. ΔF/F cutoff for activation is 0.5. Venn diagram shows that among hBD2-activated neurons, 19.05 ± 17.98% responded to serotonin. DRG, dorsal root ganglion; hBD2, human β-defensin 2; KCl, potassium chloride; WT, wild-type.



Supplementary Figure S9. Mrgpra3 neurons are not required for psoriatic inflammation. (**a**–**d**) Quantification of IMQ-induced skin pathology in WT and *Mrgpra3*^{DTA} mice across 7 days of treatment. (**a**) Skin thickness, (**b**) erythema scores, (**c**) scaling scores, and (**d**) cumulative scores from WT control (n = 6), WT IMQ (n = 6), *Mrgpra3*^{DTA} control (n = 3), and *Mrgpra3*^{DTA} IMQ (n = 5) mice across 7 days. (**e**) Representative images of shaved nape skin from WT and *Mrgpra3*^{DTA} control and IMQ-treated on days 0, 3, 5, and 7. Data are presented as mean ± SD. *$P < .05$, **$P < .01$, ***$P < .001$, and ****$P < .0001$. Two-way ANOVA was used to calculate the *P*-values. IMQ, imiquimod; WT, wild-type.



Supplementary Figure S10. Mrgprb2 is not necessary for IMQ-induced psoriatic inflammation. (**a**–**d**) Quantification of IMQ-induced skin pathology in WT and *Mrgprb2* KO mice across 7 days of treatment. (**a**) Skin thickness, **(b)** erythema scores, **(c)** scaling scores, and **(d)** cumulative scores from WT control (n = 5), WT IMQ (n = 5), *Mrgprb2* KO control (n = 4), and *Mrgprb2* KO IMQ (n = 4) mice across 7 days. (**e**) Representative images of shaved nape skin from WT and *Mrgprb2* KO control and IMQ-treated on days 0 and 7. Data are presented as mean ± SD. Two-way ANOVA was used to calculate the *P*-values. IMQ, imiquimod; KO, knockout; WT, wild-type.